Laboratoř růstových regulátorů

Miroslav Strnad

Fyziologie rostlinné buňky , cytoskelet, buněčné dělení a onkogeneze [kap 1]

- Univerzita Palackého & Ústav experimentální botaniky AV CR

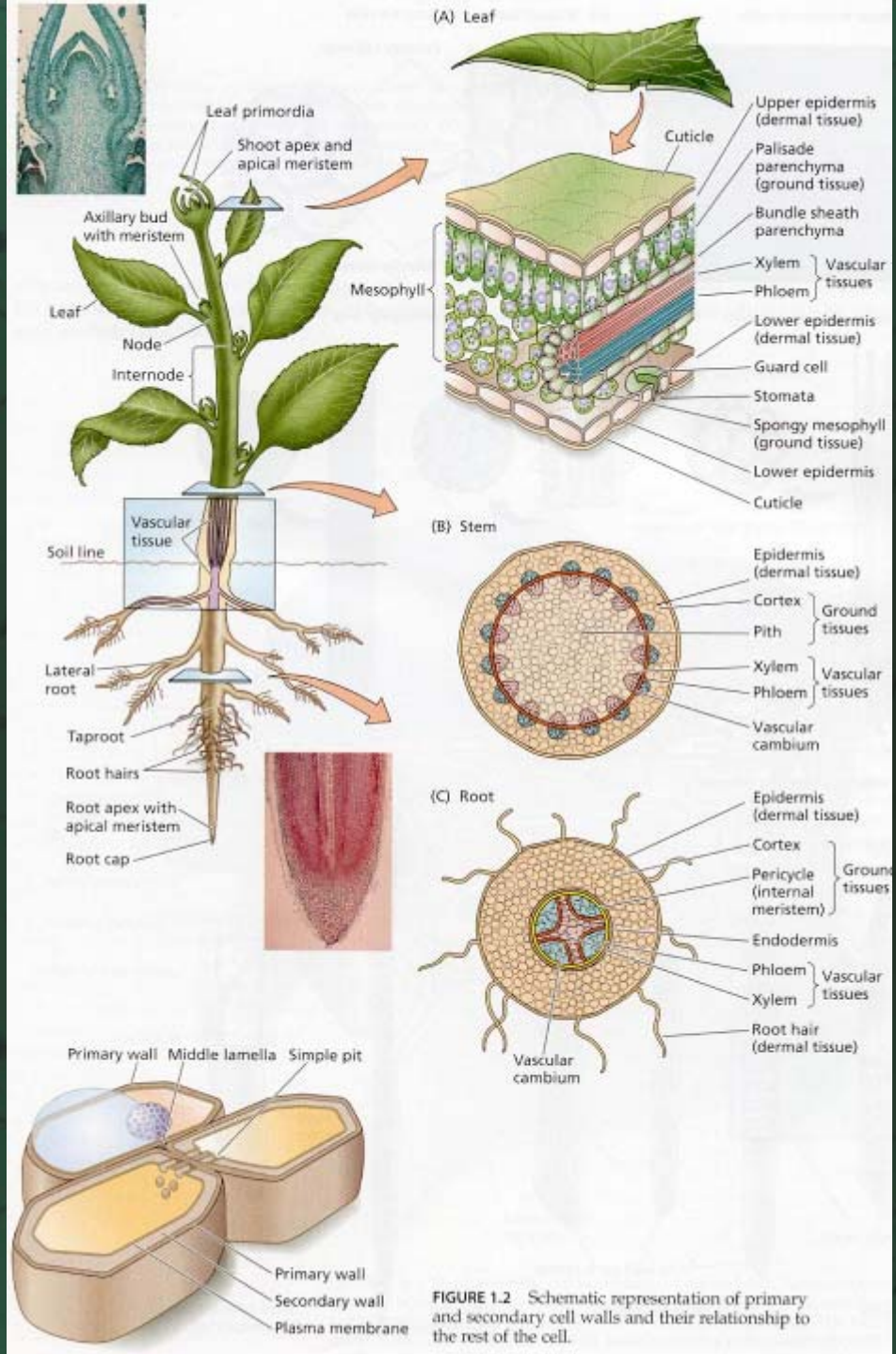

FIGURE 1.2 Schematic representation of primary and secondary cell walls and their relationship to the rest of the cell.

(A) Dermal tissue: epidermal cells

(B) Ground tissue: parenchyma cells

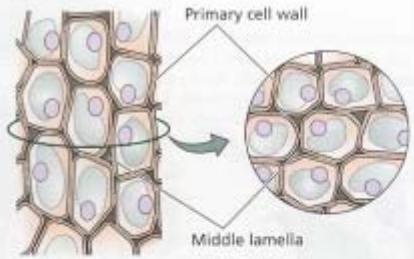

(C) Ground tissue: collenchyma cells

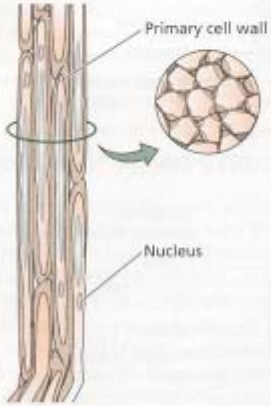

(D) Ground tissue: sclerenchyma cells

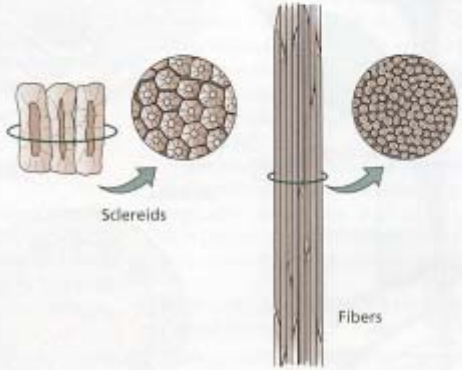

(E) Vascular tisssue: xylem and phloem

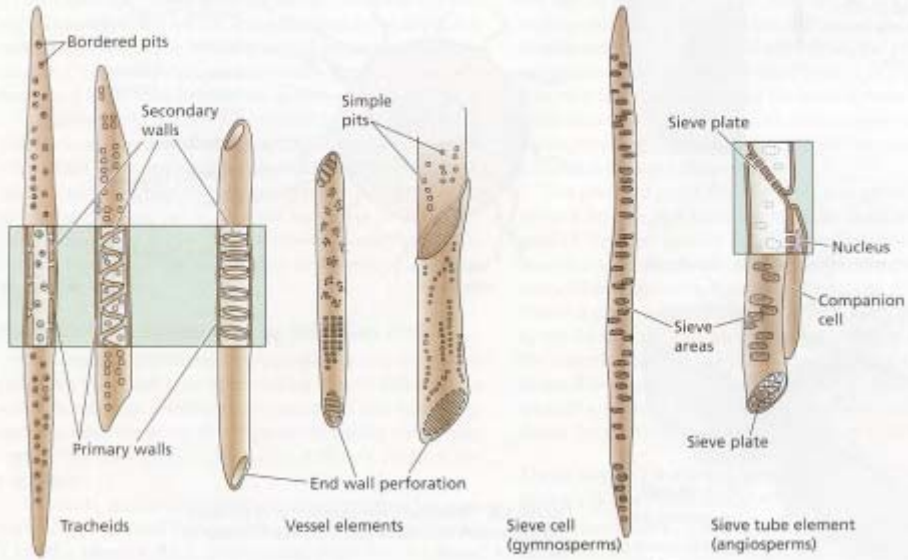

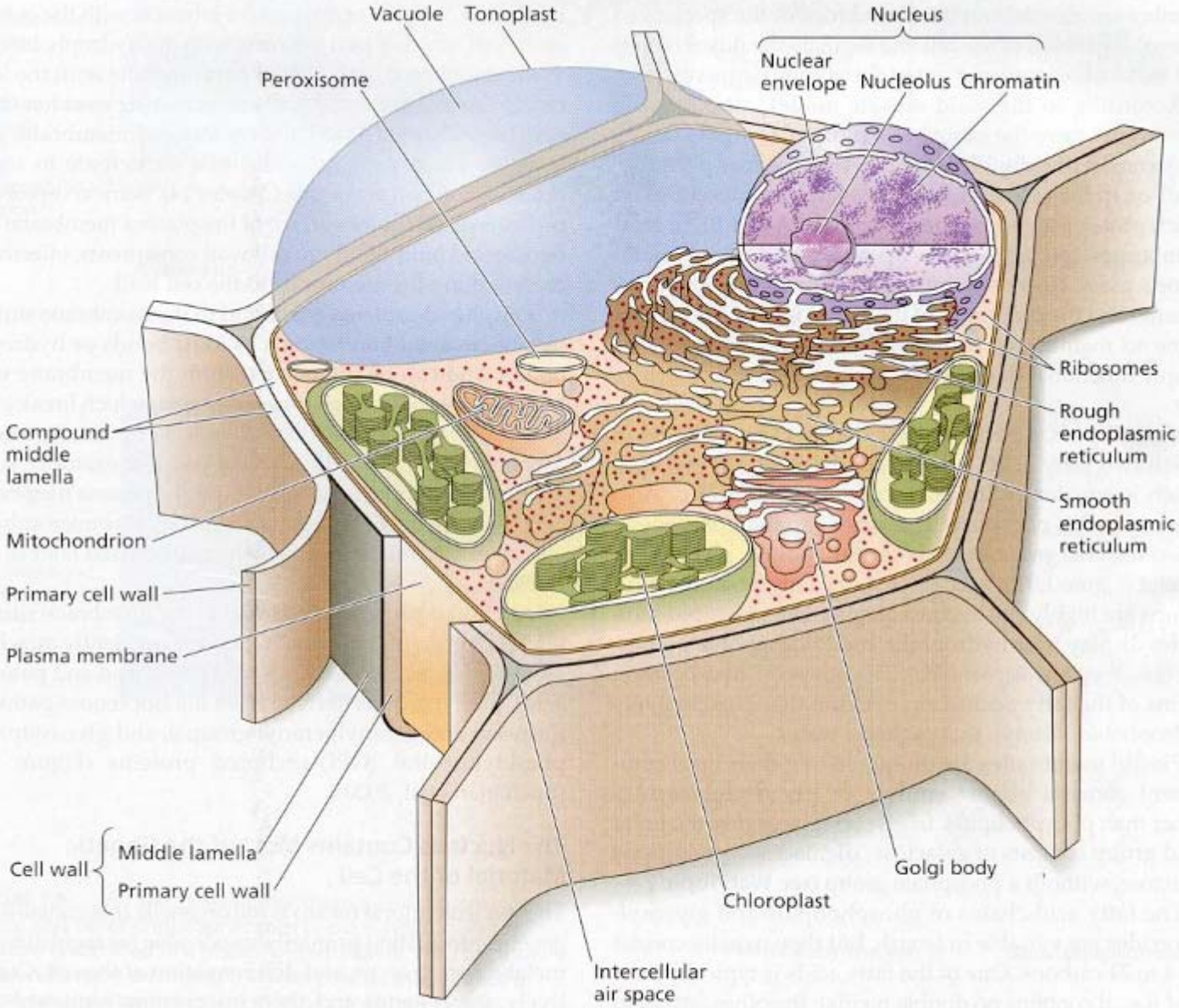

FIGURE 1.4 Diagrammatic representation of a plant cell. Various intracellular compartments are defined by their respective membranes, such as the tonoplast, the nuclear envelope, and the membranes of the other organelles. The two adjacent primary walls, along with the middle lamella, form a composite structure called the compound middle lamella.

(A)

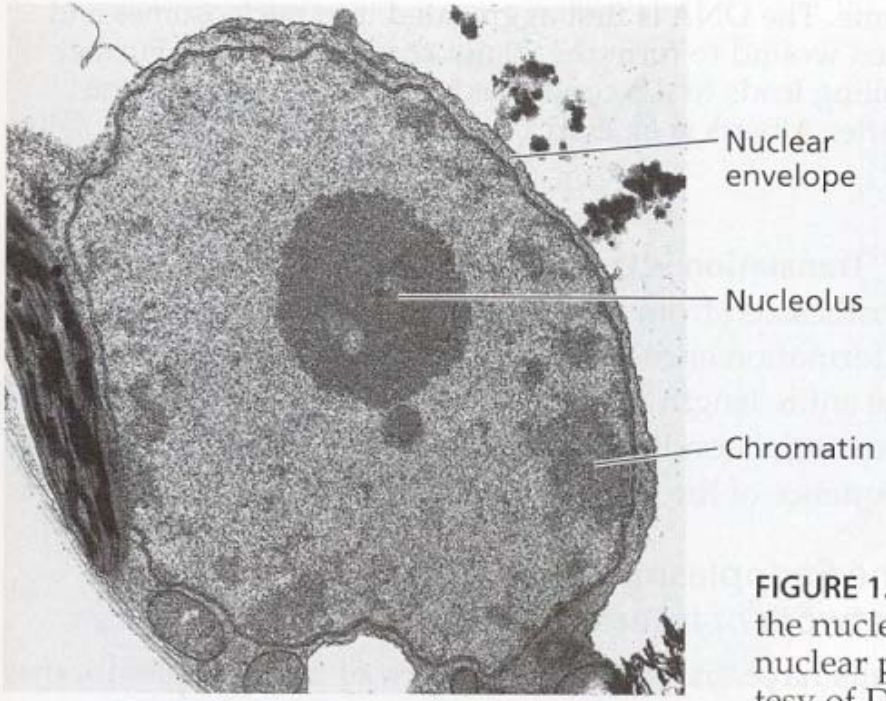

(B)

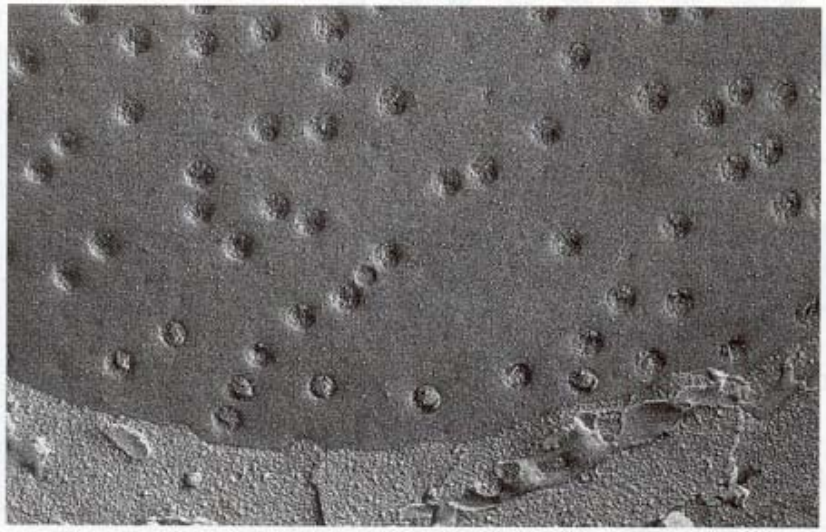

FIGURE 1.7 (A) Transmission electron micrograph of a plant cell, showing the nucleolus and the nuclear envelope. (B) Freeze-etched preparation of nuclear pores from a cell of an onion root. (A courtesy of R. Evert; B courtesy of D. Branton.)

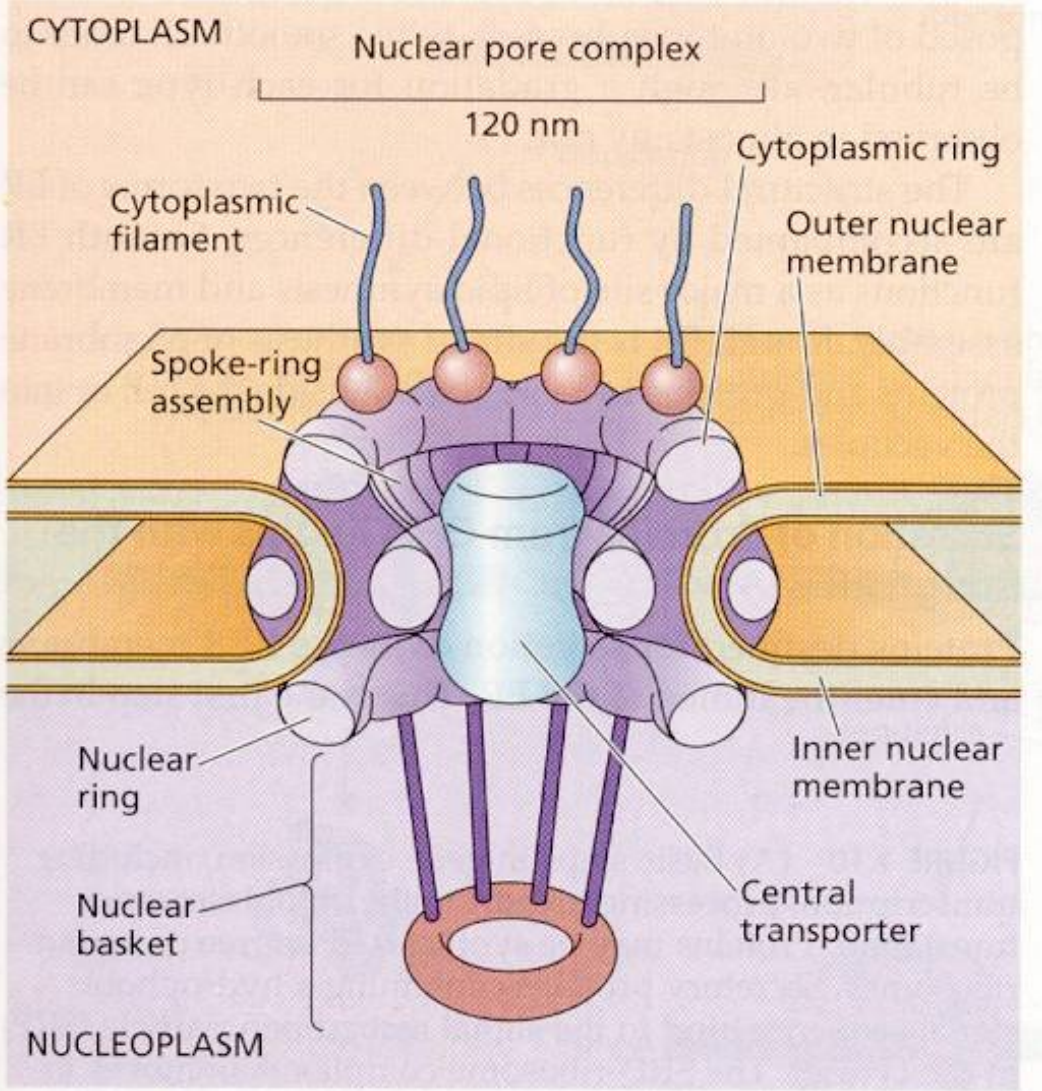

FIGURE 1.8 Schematic model of the structure of the nuclear pore complex. Parallel rings composed of eight subunits each are arranged octagonally near the inner and outer membranes of the nuclear envelope. Various proteins form the other structures, such as the nuclear ring, the spoke-ring assembly, the central transporter, the cytoplasmic filaments, and the nuclear basket.

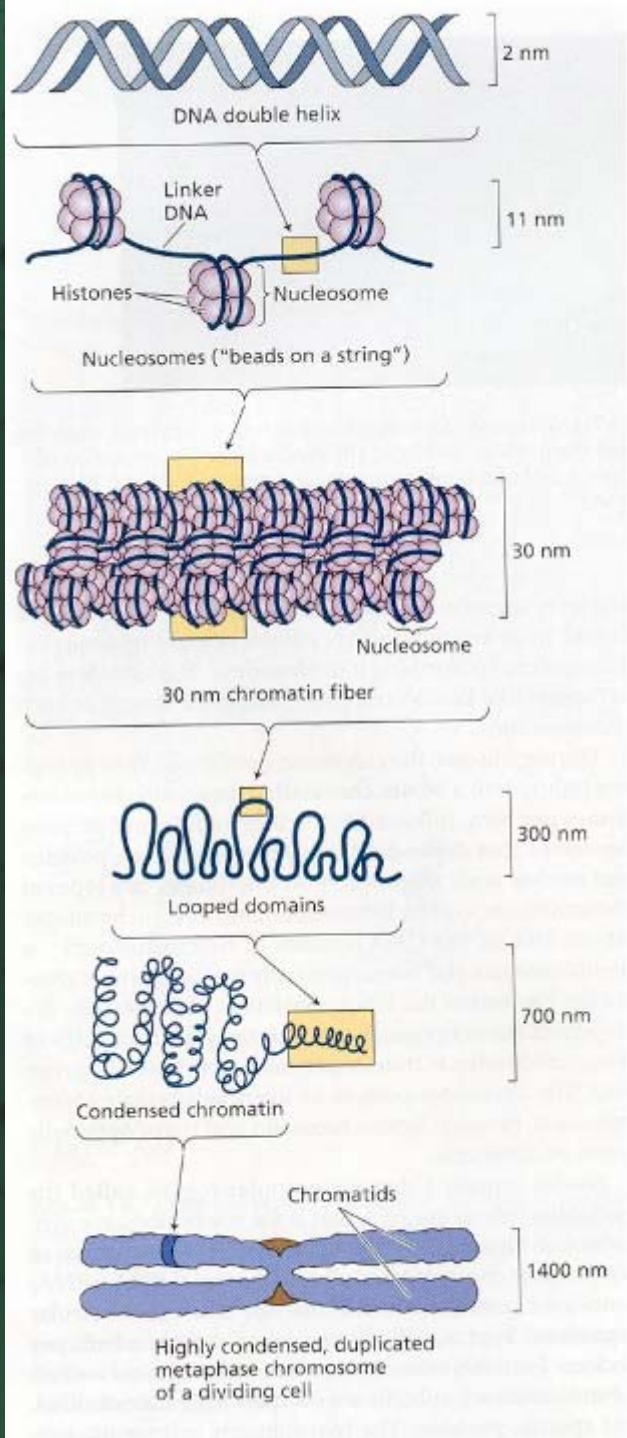

FIGURE 1.9 Packaging of DNA in a metaphase chromosome. The DNA is first aggregated into nucleosomes and then wound to form the 30 nm chromatin fibers. Further coiling leads to the condensed metaphase chromosome. (After Alberts et al. 2002.)

ER má rezidentní bílkoviny – retikuloplasminy – retenční signál HDEL (homologa HSP70), retrográdním způsobem vraceny do ER, bez správného konformace jsou proteiny degradovány protesomem v cytoplasmě

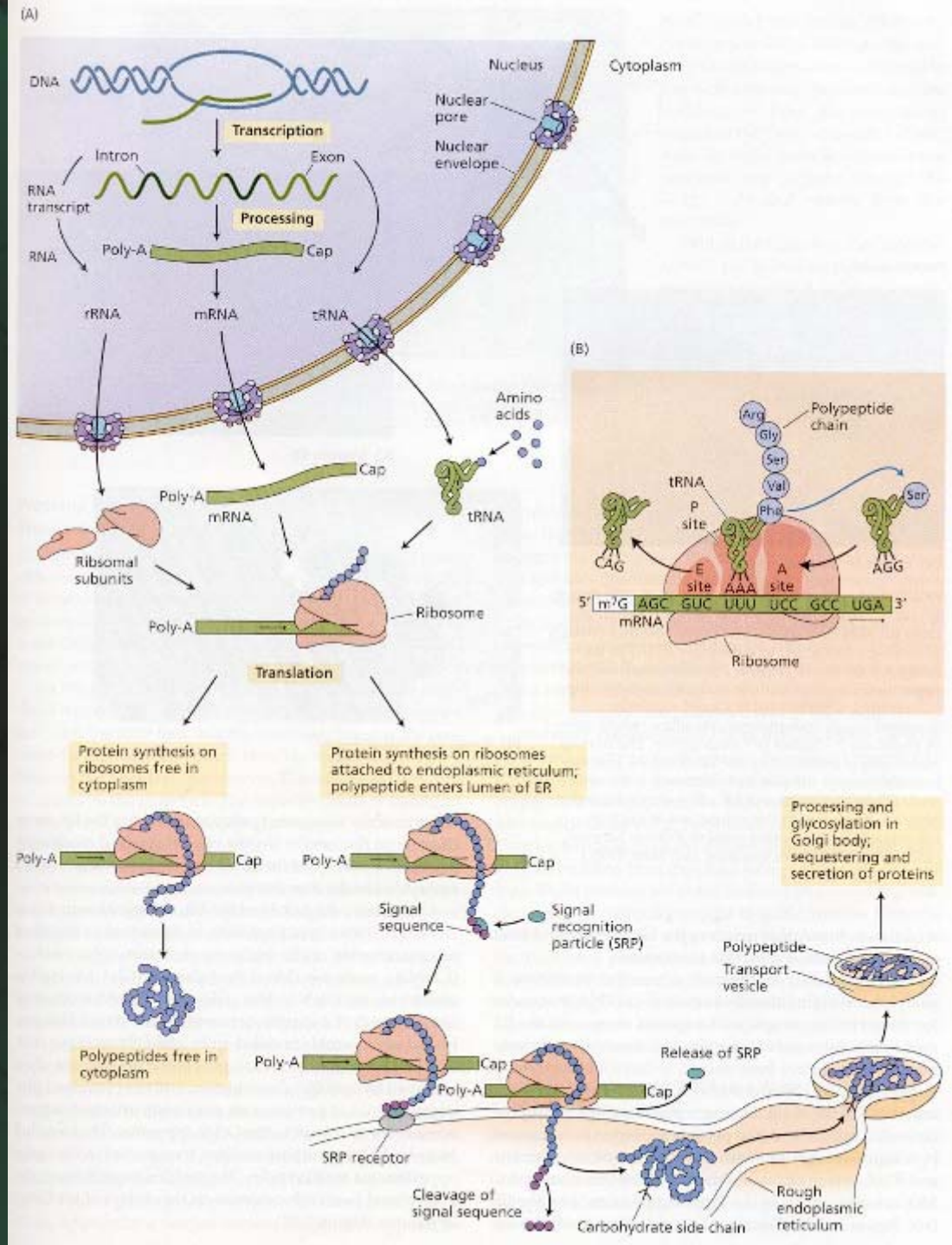

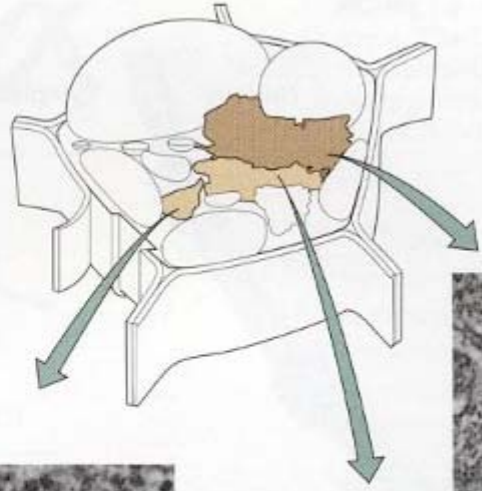

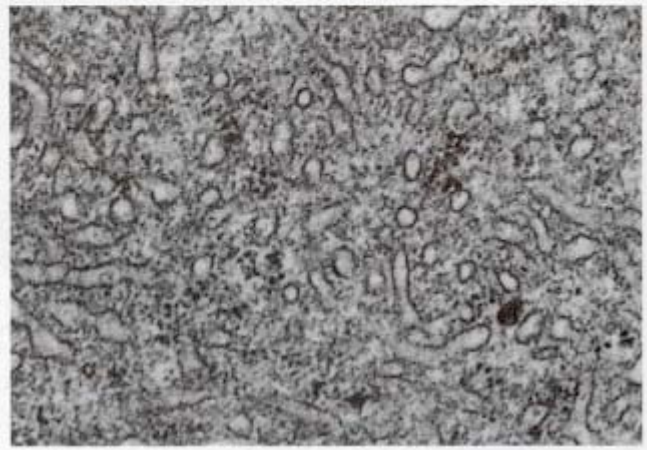

(C) Smooth ER

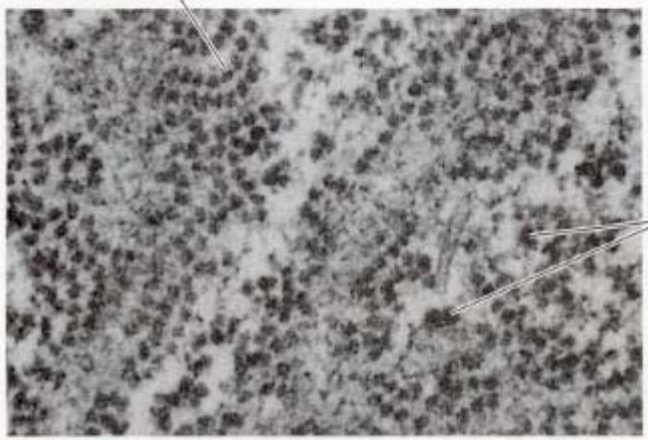

(A) Rough ER (surface view)

(B) Rough ER (cross section)

FIGURE 1.11 The endoplasmic reticulum. (A) Rough ER can be seen in surface view in this micrograph from the alga *Bulbochaete*. The polyribosomes (strings of ribosomes attached to messenger RNA) in the rough ER are clearly visible. Polyribosomes are also present on the outer surface of the nuclear envelope (N-nucleus). (75,000×) (B) Stacks of regularly arranged rough endoplasmic reticulum (white arrow) in glandular trichomes of *Coleus blumei*. The plasma membrane is indicated by the black arrow, and the material outside the plasma membrane is the cell wall. (75,000×) (C) Smooth ER often forms a tubular network, as shown in this transmission electron micrograph from a young petal of *Primula kewensis*. (45,000×) (Photos from Gunning and Steer 1996.)

transfer of the elongating polypeptide across the ER membrane into the lumen. (In the case of integral membrane proteins, a portion of the completed polypeptide remains

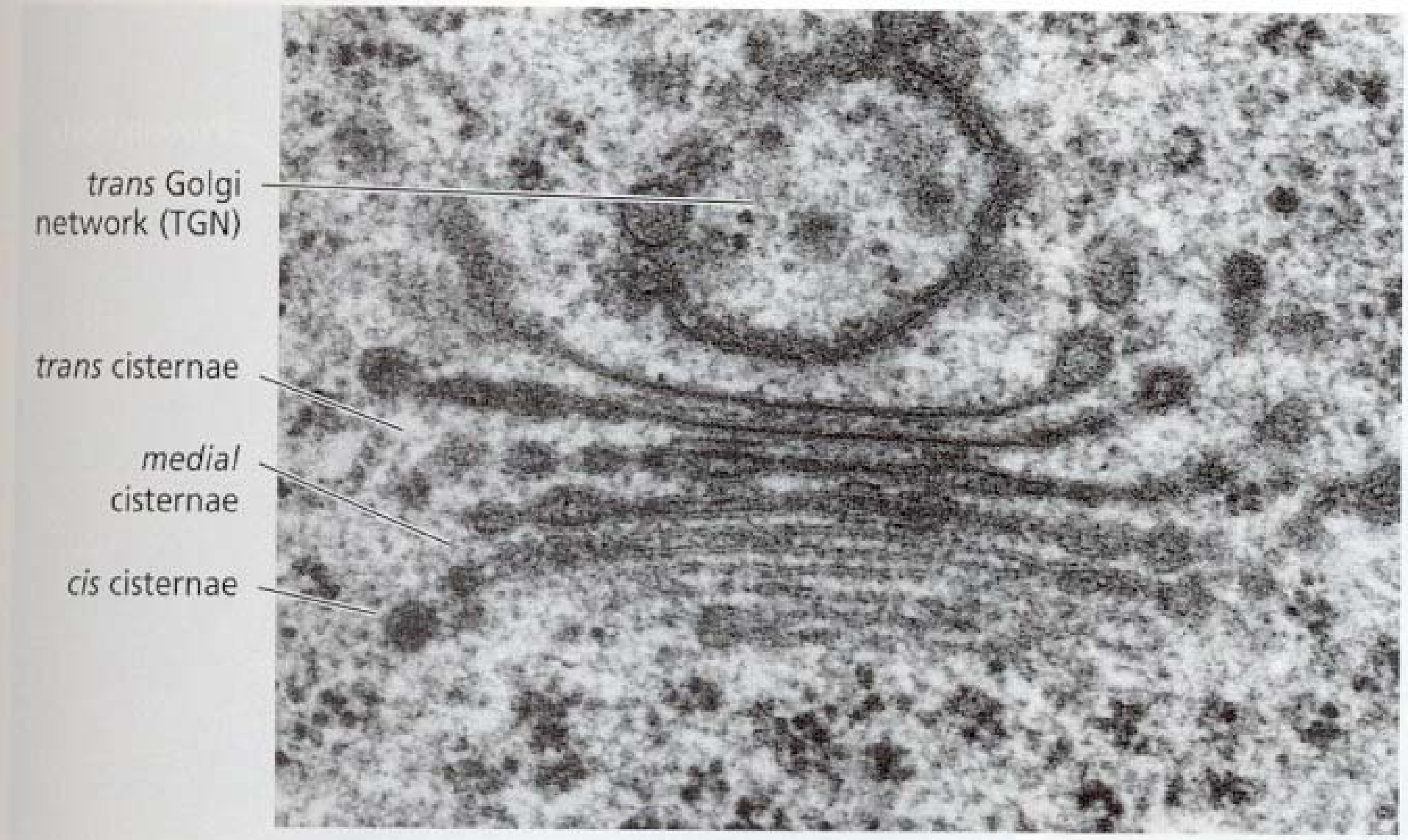

FIGURE 1.12 Electron micrograph of a Golgi apparatus in a tobacco (*Nicotiana tabacum*) root cap cell. The *cis*, *medial*, and *trans* cisternae are indicated. The *trans* Golgi network is associated with the *trans* cisterna. (60,000×) (From Gunning and Steer 1996.)

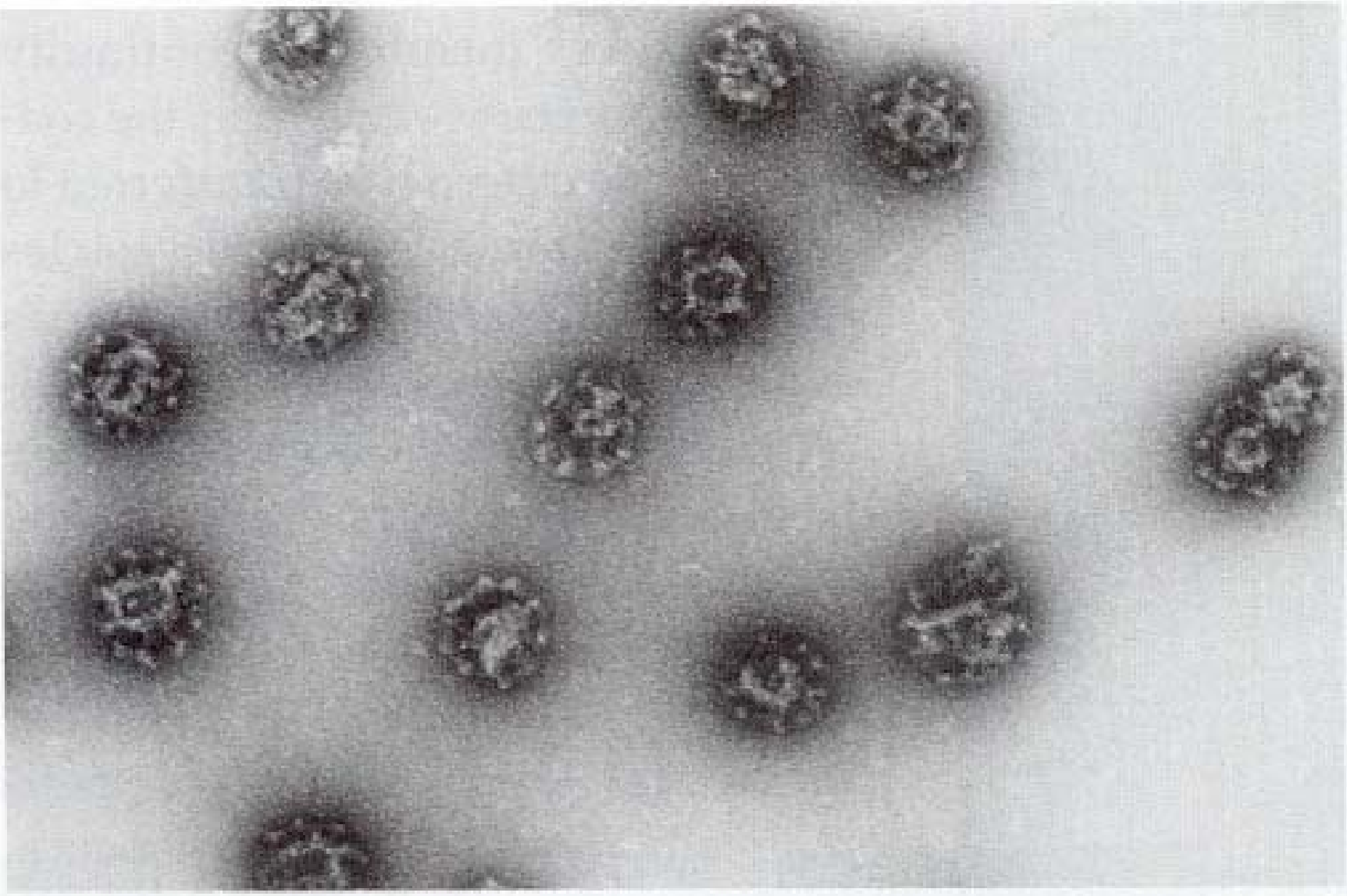

FIGURE 1.13 Preparation of clathrin-coated vesicles isolated from bean leaves. (102,000×) (Photo courtesy of D. G. Robinson.)

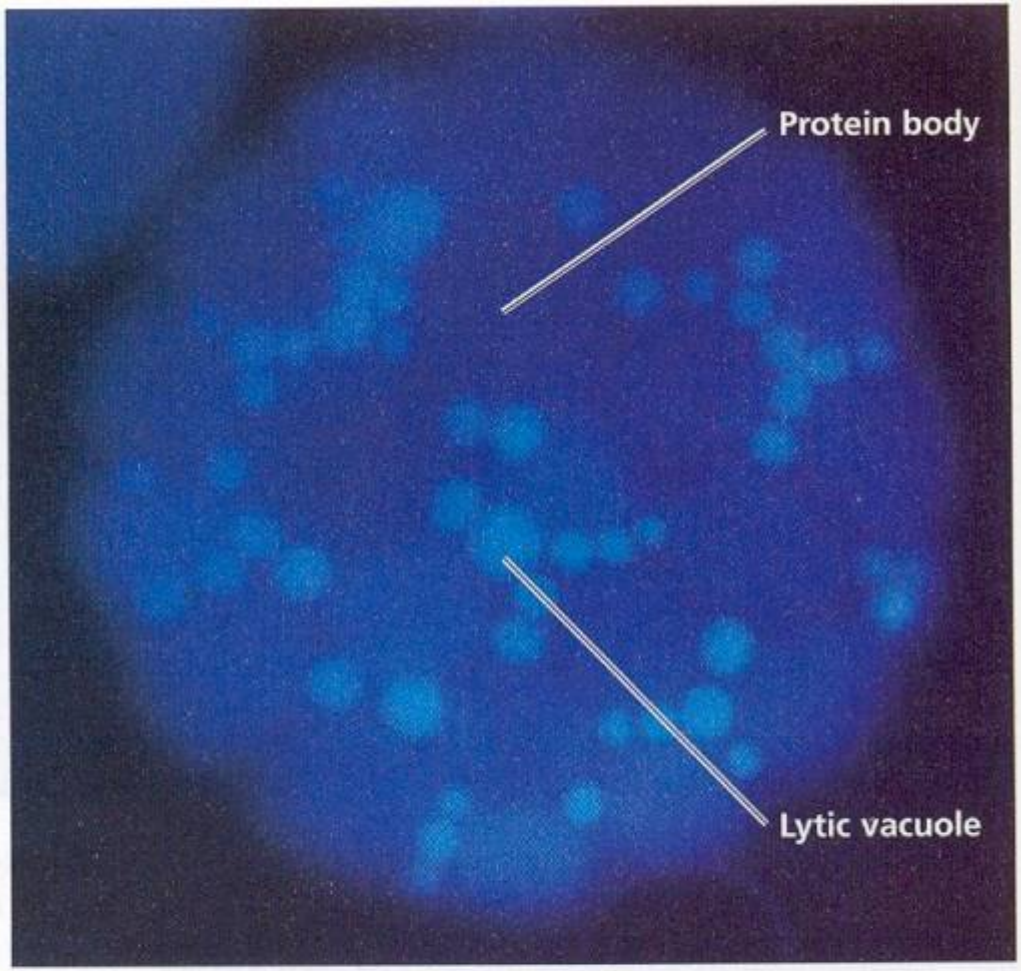

FIGURE 1.14 Light micrograph of a protoplast prepared from the aleurone layer of seeds. The fluorescent stain reveals two types of vacuoles: the larger protein bodies (V_1) and the smaller lytic vacuoles (V_2). (Photo courtesy of P. Bethke and R. L. Jones.)

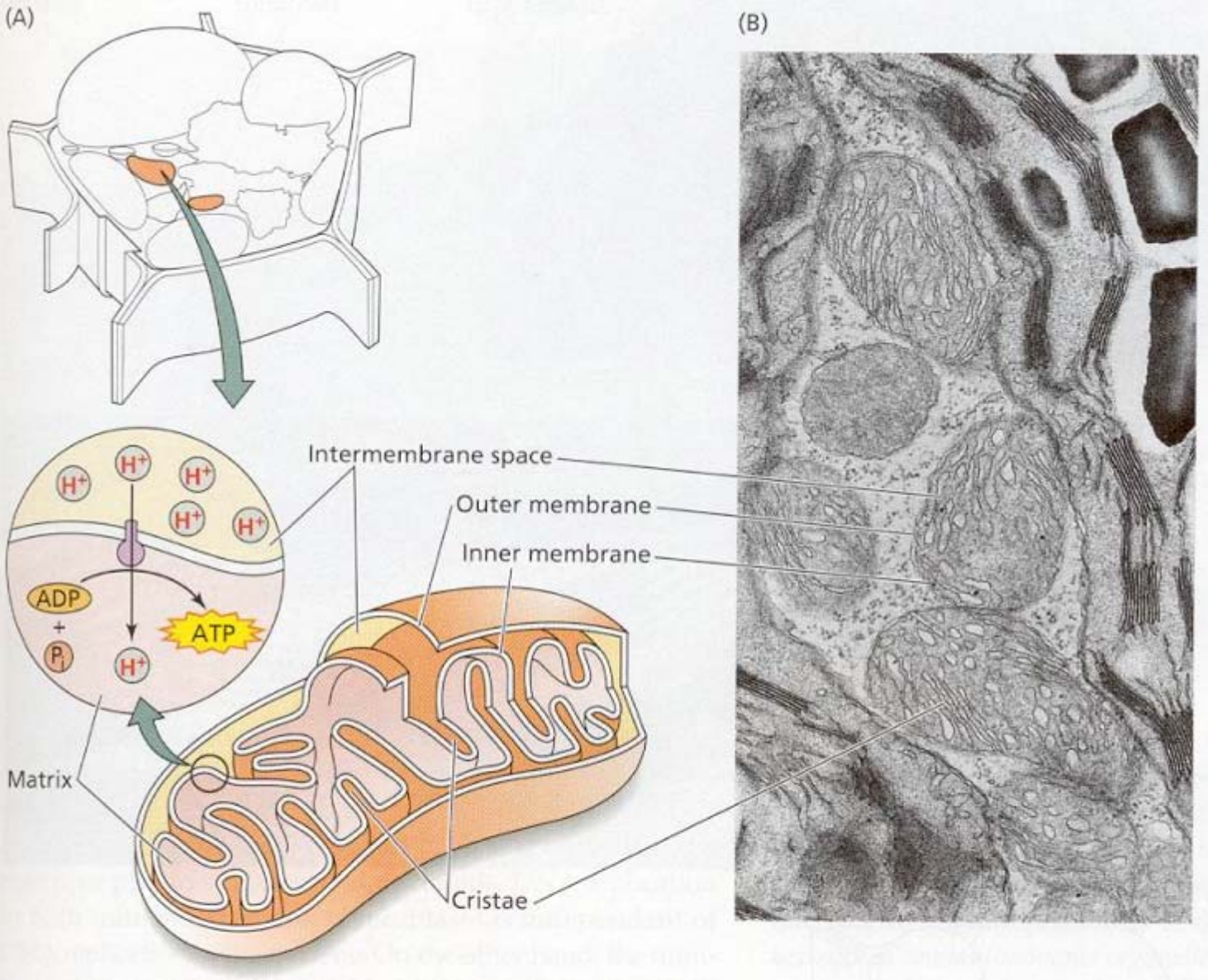

FIGURE 1.15 (A) Diagrammatic representation of a mitochondrion, including the location of the H^+-ATPases involved in ATP synthesis on the inner membrane. (B) An electron micrograph of mitochondria from a leaf cell of Bermuda grass, *Cynodon dactylon*. (26,000×) (Photo by S. E. Frederick, courtesy of E. H. Newcomb.)

result in a proton gradient across the
As in the mitochondria, ATP is synt

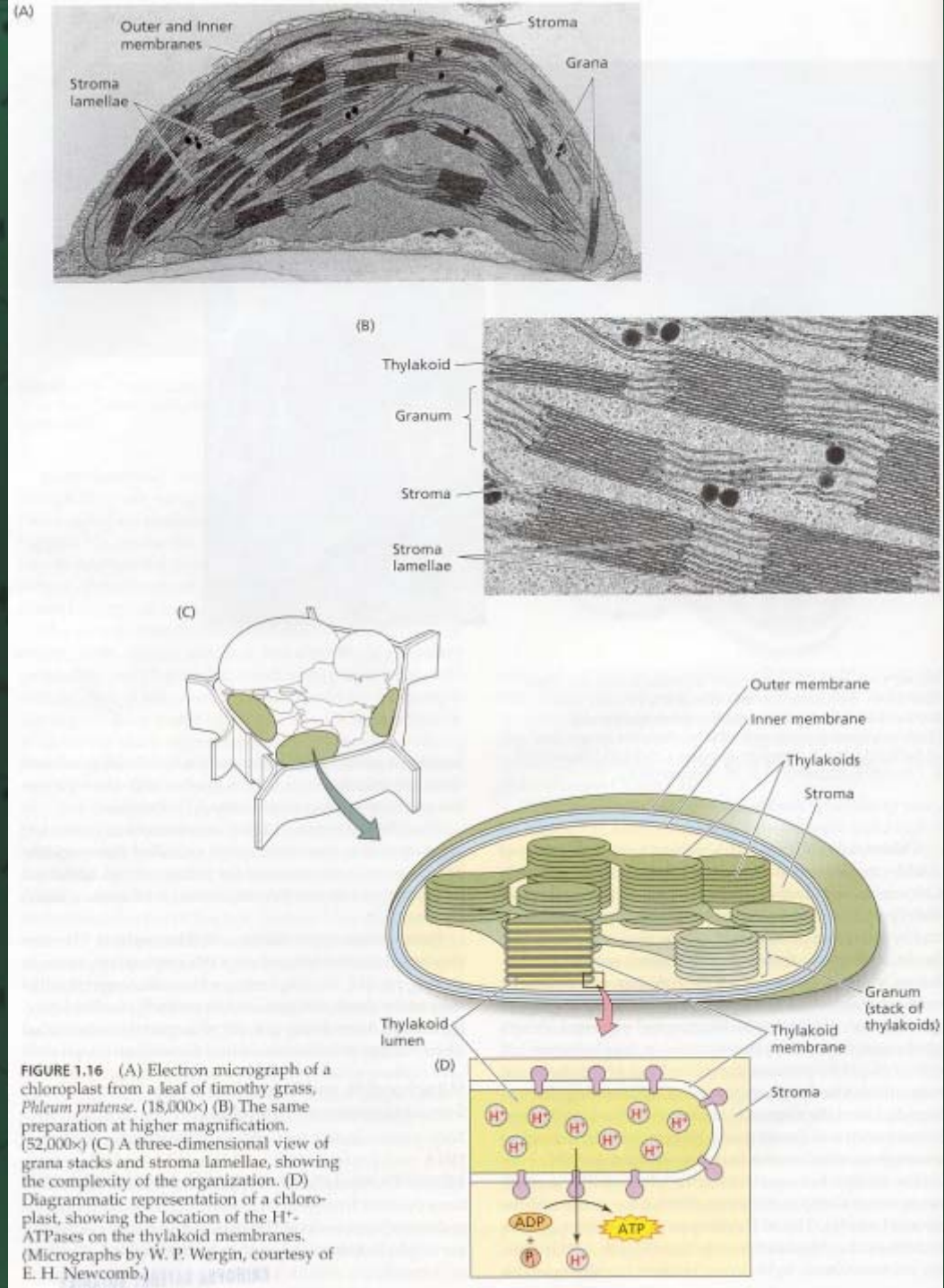

FIGURE 1.16 (A) Electron micrograph of a chloroplast from a leaf of timothy grass, *Phleum pratense*. (18,000×) (B) The same preparation at higher magnification. (52,000×) (C) A three-dimensional view of grana stacks and stroma lamellae, showing the complexity of the organization. (D) Diagrammatic representation of a chloroplast, showing the location of the H^+-ATPases on the thylakoid membranes. (Micrographs by W. P. Wergin, courtesy of E. H. Newcomb.)

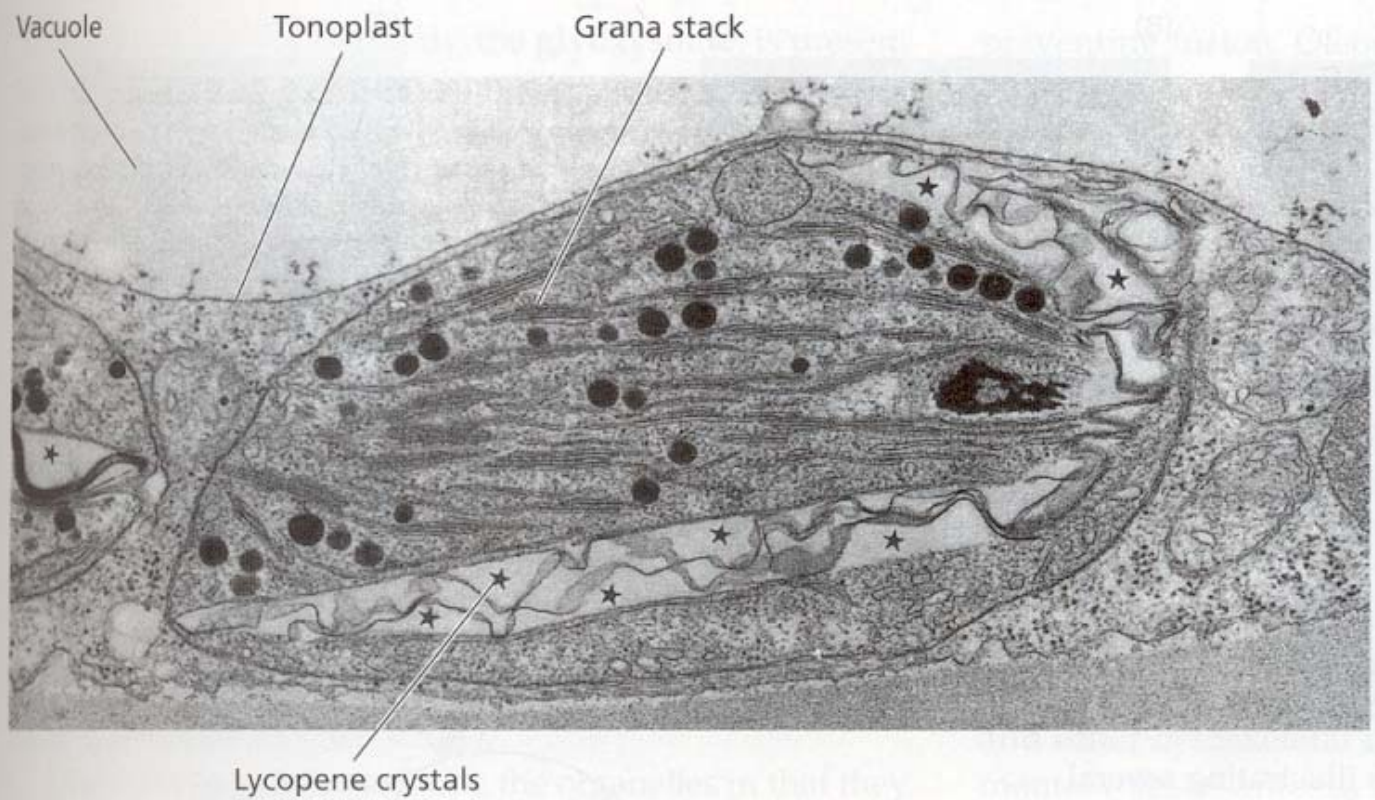

FIGURE 1.17 Electron micrograph of a chromoplast from tomato (*Lycopersicon esculentum*) fruit at an early stage in the transition from chloroplast to chromoplast. Small grana stacks are still visible. Crystals of the carotenoid lycopene are indicated by the stars. (27,000×) (From Gunning and Steer 1996.)

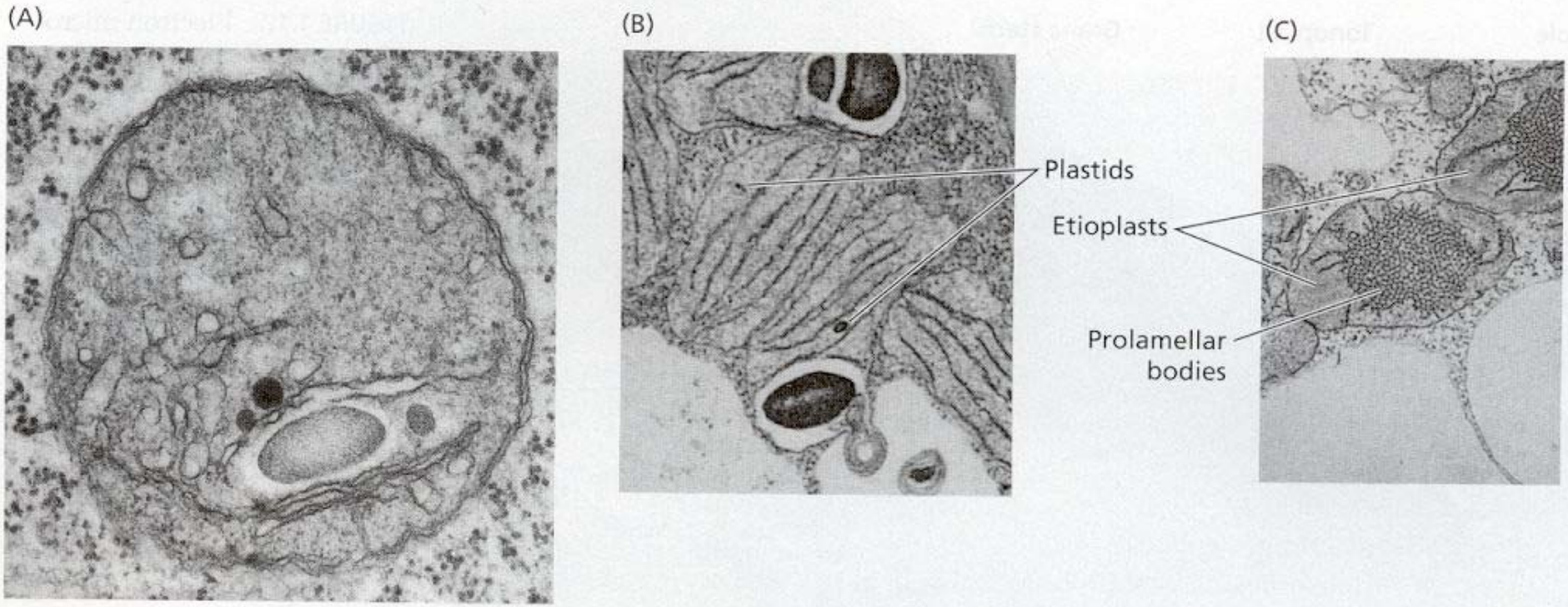

FIGURE 1.18 Electron micrographs illustrating several stages of plastid development. (A) A higher-magnification view of a proplastid from the root apical meristem of the broad bean (*Vicia faba*). The internal membrane system is rudimentary, and grana are absent. (47,000×) (B) A mesophyll cell of a young oat leaf at an early stage of differentiation in the light. The plastids are developing grana stacks. (C) A cell from a young oat leaf from a seedling grown in the dark. The plastids have developed as etioplasts, with elaborate semicrystalline lattices of membrane tubules called prolamellar bodies. When exposed to light, the etioplast can convert to a chloroplast by the disassembly of the prolamellar body and the formation of grana stacks. (7,200×) (From Gunning and Steer 1996.)

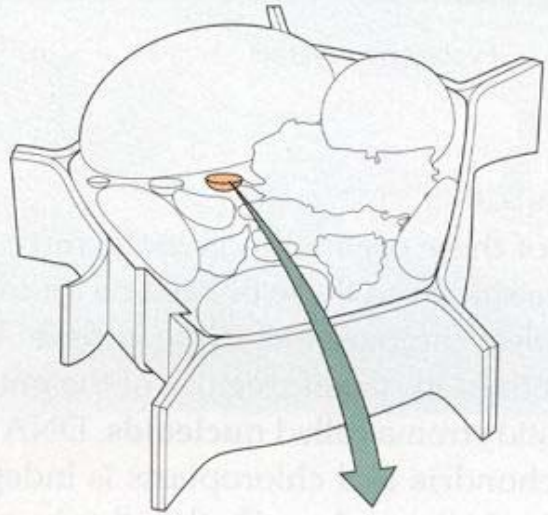

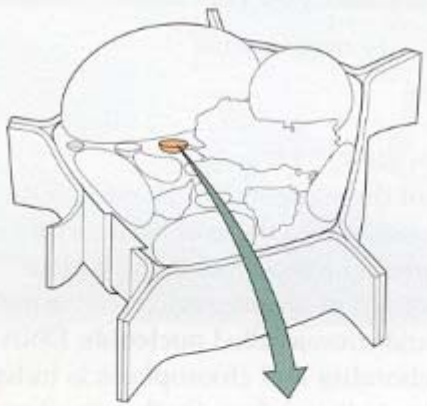

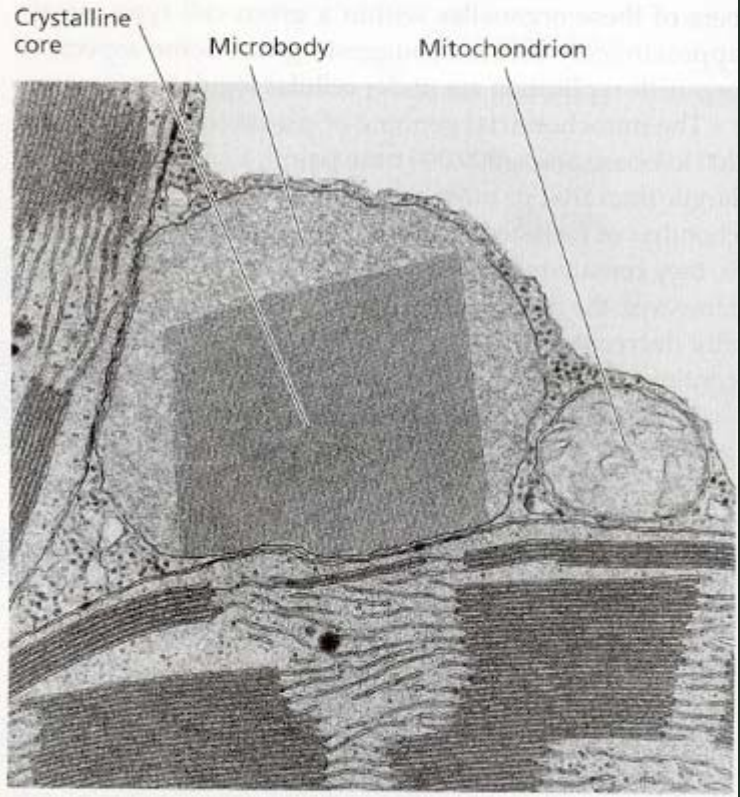

FIGURE 1.19 Electron micrograph of a peroxisome from a mesophyll cell, showing a crystalline core. (27,000×) This peroxisome is seen in close association with two chloroplasts and a mitochondrion, probably reflecting the cooperative role of these three organelles in photorespiration. (From Huang 1987.)

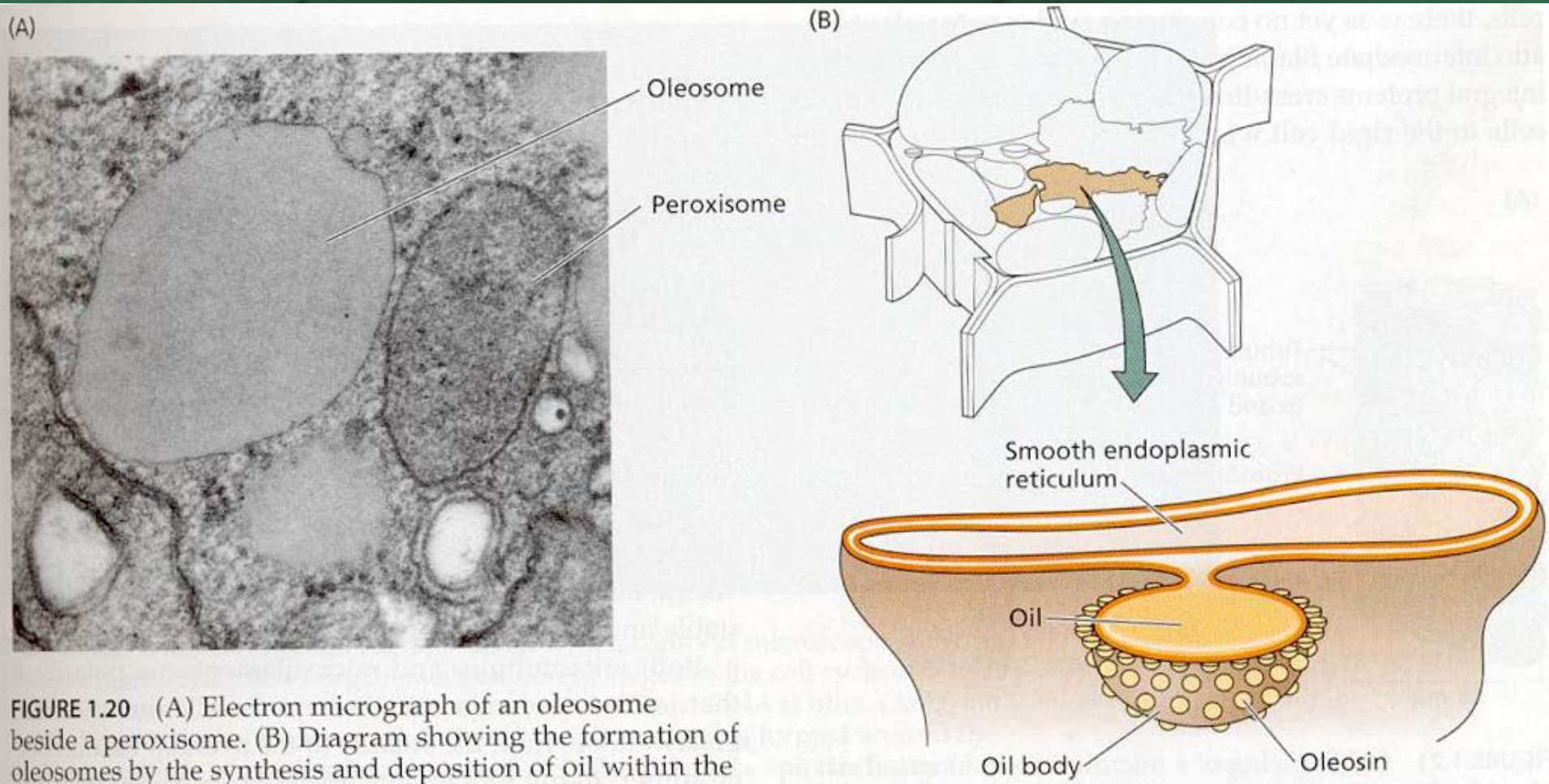

FIGURE 1.20 (A) Electron micrograph of an oleosome beside a peroxisome. (B) Diagram showing the formation of oleosomes by the synthesis and deposition of oil within the phospholipid bilayer of the ER. After budding off from the ER, the oleosome is surrounded by a phospholipid monolayer containing the protein oleosin. (A from Huang 1987; B after Buchanan et al. 2000.)

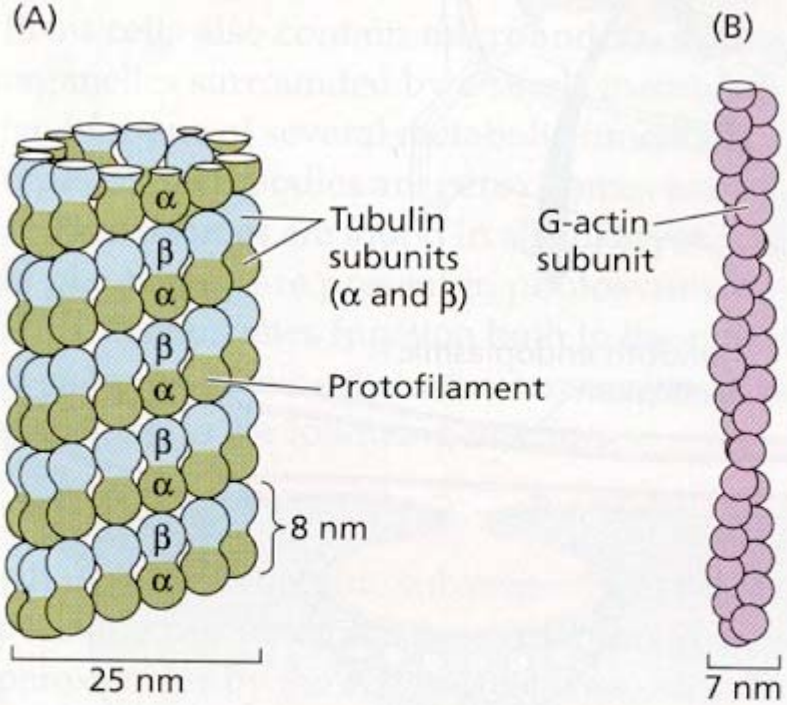

FIGURE 1.21 (A) Drawing of a microtubule in longitudinal view. Each microtubule is composed of 13 protofilaments. The organization of the α and β subunits is shown. (B) Diagrammatic representation of a microfilament, showing two strands of G-actin subunits.

Mikrotubulární cytoskelet

α a β–tubulin u rostlin

Mikrotubulární organizační centra – MTOCs – na plazmalemě a jaderné membráně, vyšší rostliny nemají centrosom (centrioly), v přechodu do mitosy na jaderné membráně, hlavně γ–tubulin

MAPs – bílkoviny asociované s mikrotubuly

velmi typické pro rostliny, napojení cytoskeletu na membrány, zvyšují odolnost vůči chladu, reguluje MAP - fosfolipasa D, kateniny – štěpí miktrotubuly na fragmenty

Mirkotubulární motory – slouží k vnitrobuněčnému transportu váčků po povrchu cytoskeletu, ATP, pouze v jednom směru, kinesin (od - k + konci) místo dyneinu

Aktinový cytoskelet

F-aktinová mikrofilamenta u rostlin, F-aktin (fibrilární), z G-aktinu (globulární), váže ATP a profilin skládá mikrofilamenta

ARPs – bílkoviny asociované s aktinem, ADF – faktory depolimerující aktin

Aktinové motory – slouží k vnitrobuněčnému transportu váčků po povrchu cytoskeletu, ATP, pouze v jednom směru, myosiny, indukují proudění cytoplasmy (cyklosa), často vázán na mikrotubuly- stabilizace

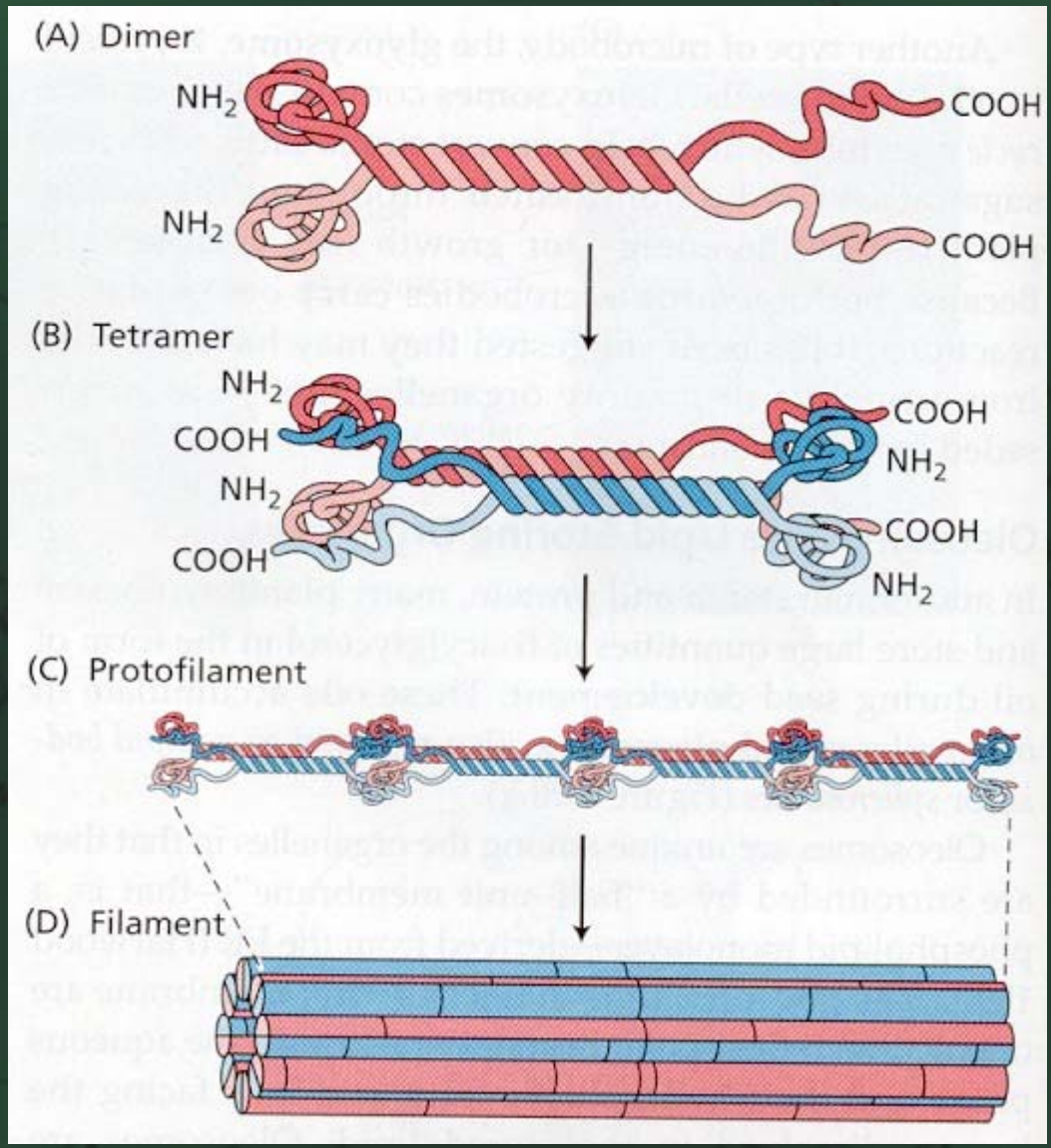
(A) Dimer
NH2
COOH
NH2
COOH
(B) Tetramer
NH2
COOH
NH2
COOH
COOH
NH2
COOH
NH2
(C) Protofilament
(D) Filament

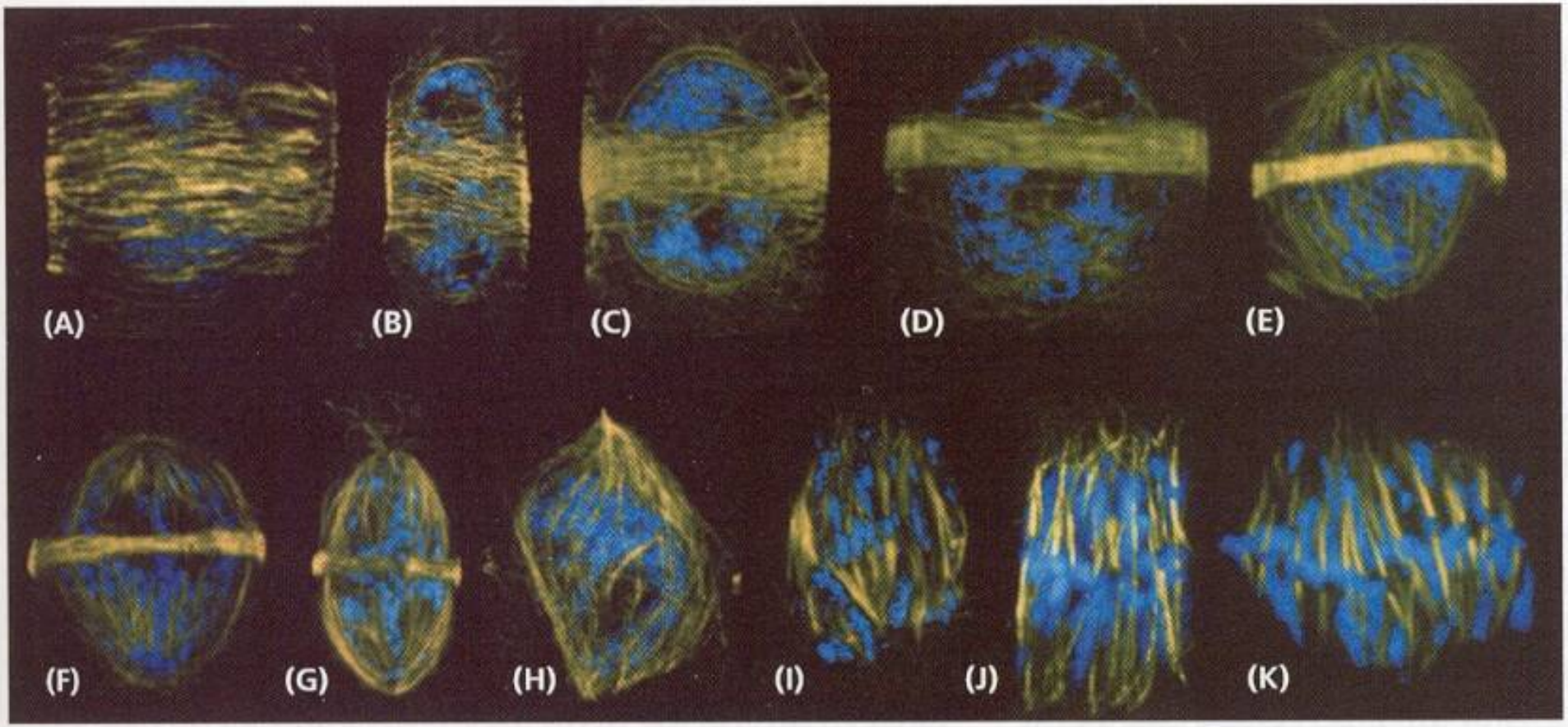

FIGURE 1.23 Fluorescence micrograph taken with a confocal microscope showing changes in microtubule arrangements at different stages in the cell cycle of wheat root meristem cells. Microtubules stain green and yellow; DNA is blue. (A–D) Cortical microtubules disappear and the preprophase band is formed around the nucleus at the site of the future cell plate. (E–H) The prophase spindle forms from foci of microtubules at the poles. (G, H) The preprophase band disappears in late prophase. (I–K) The nuclear membrane breaks down, and the two poles become more diffuse. The mitotic spindle forms in parallel arrays and the kinetochores bind to spindle microtubules. (From Gunning and Steer 1996.)

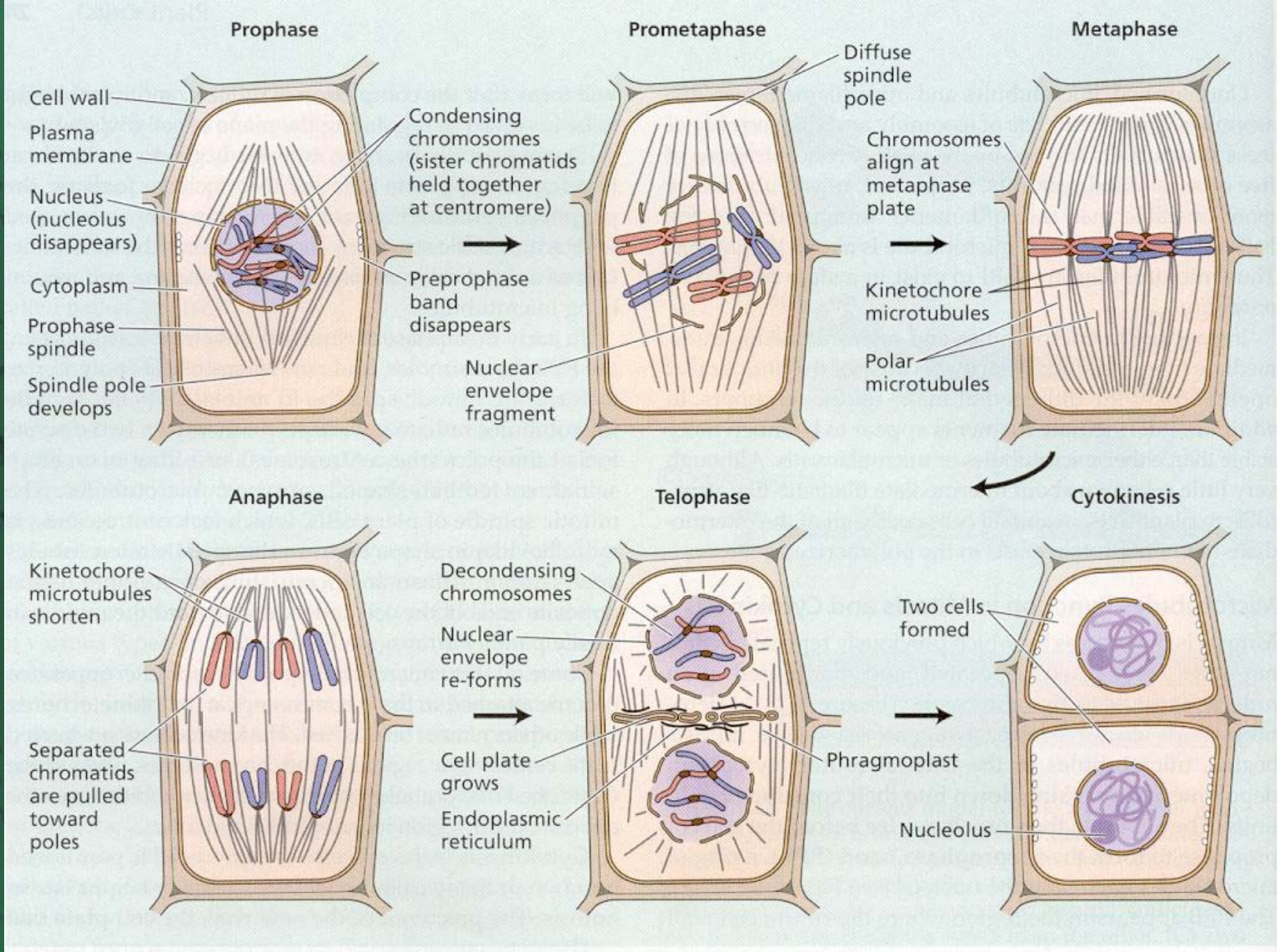

FIGURE 1.24 Diagram of mitosis in plants.

Cell cycle

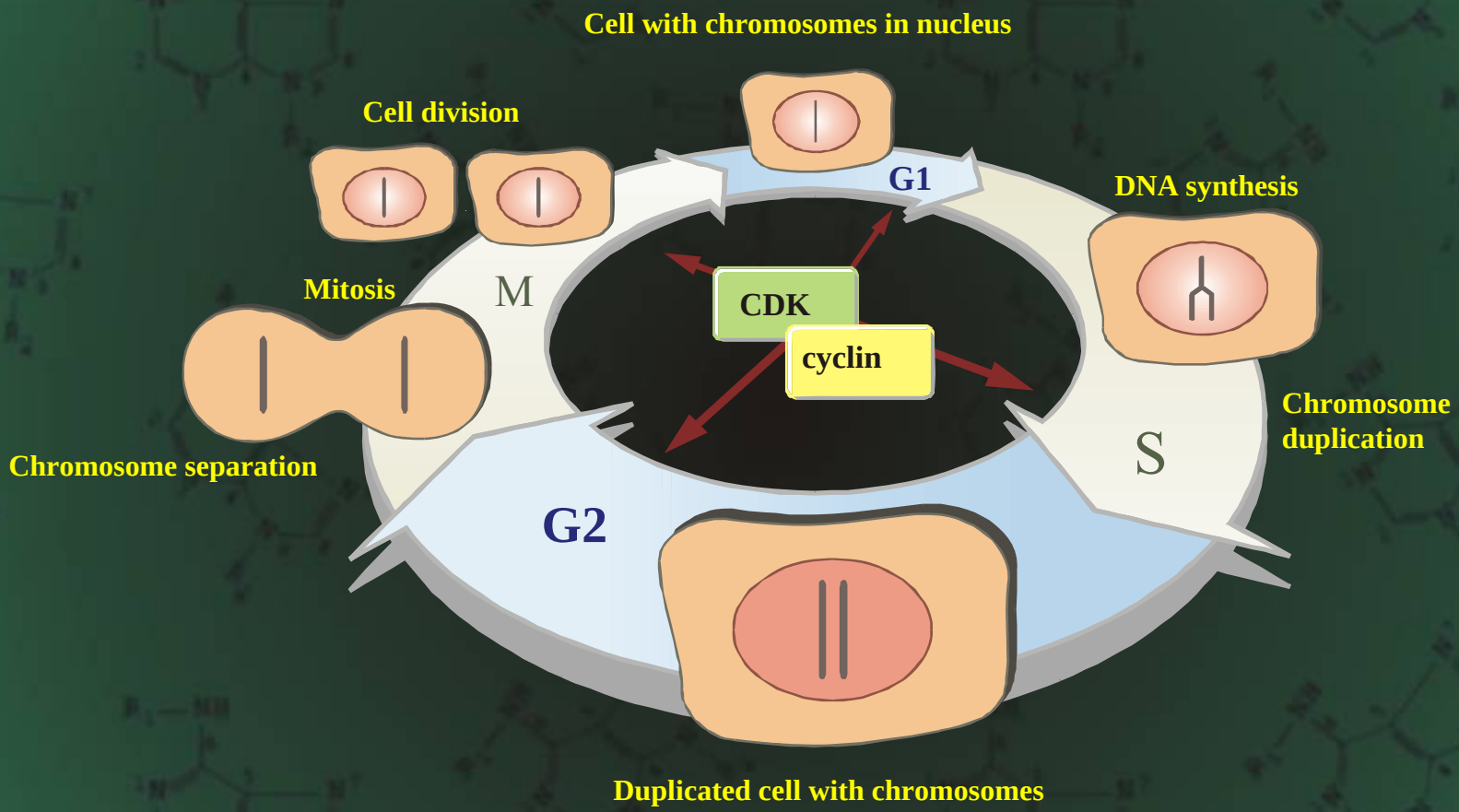
Cell with chromosomes in nucleus
Cell division
G1
DNA synthesis
Mitosis
M
CDK
cyclin
Chromosome separation
S
Chromosome duplication
G2
Duplicated cell with chromosomes

Regulation of CDK activity

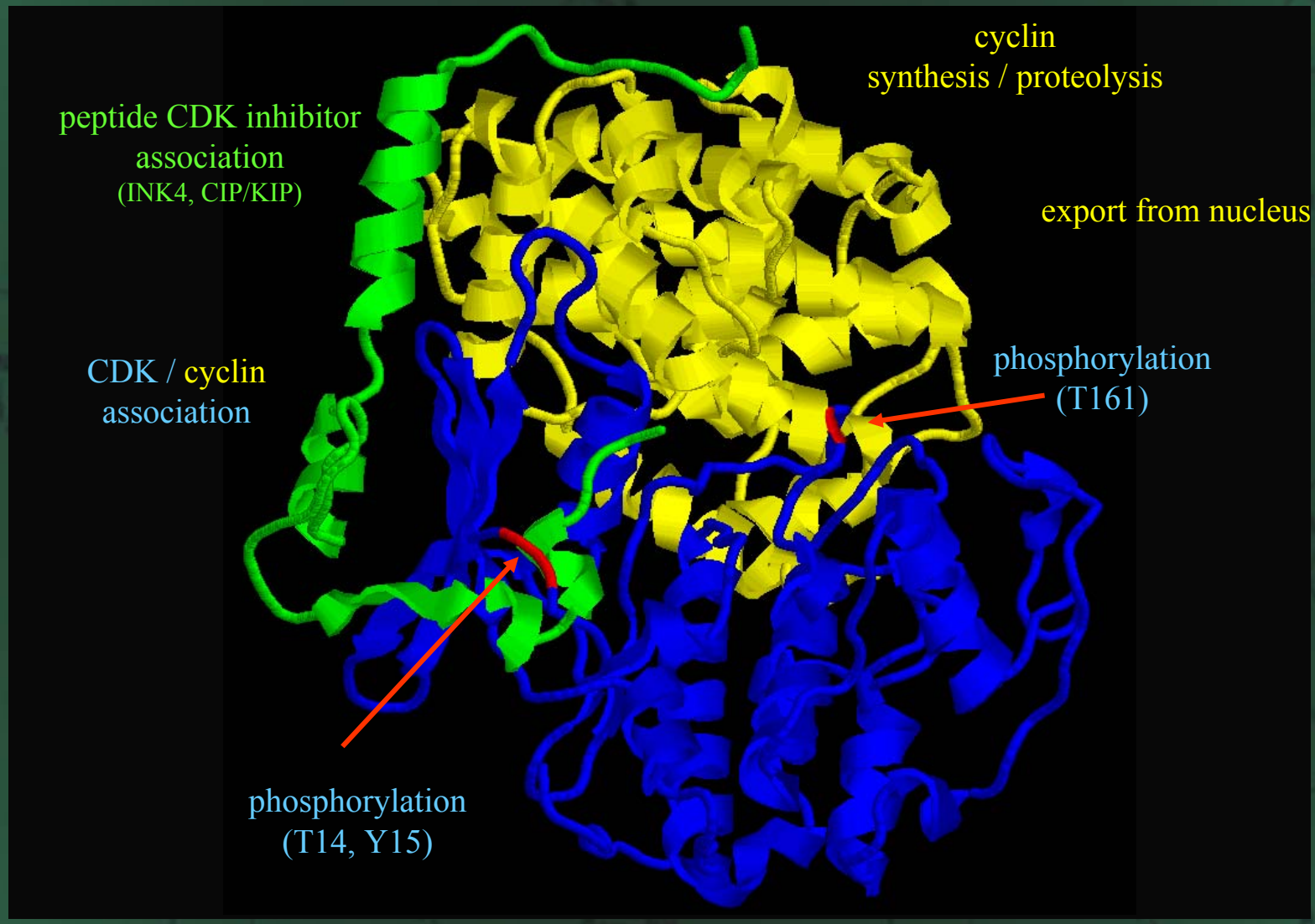

Regulation of CDK activity by cyclins

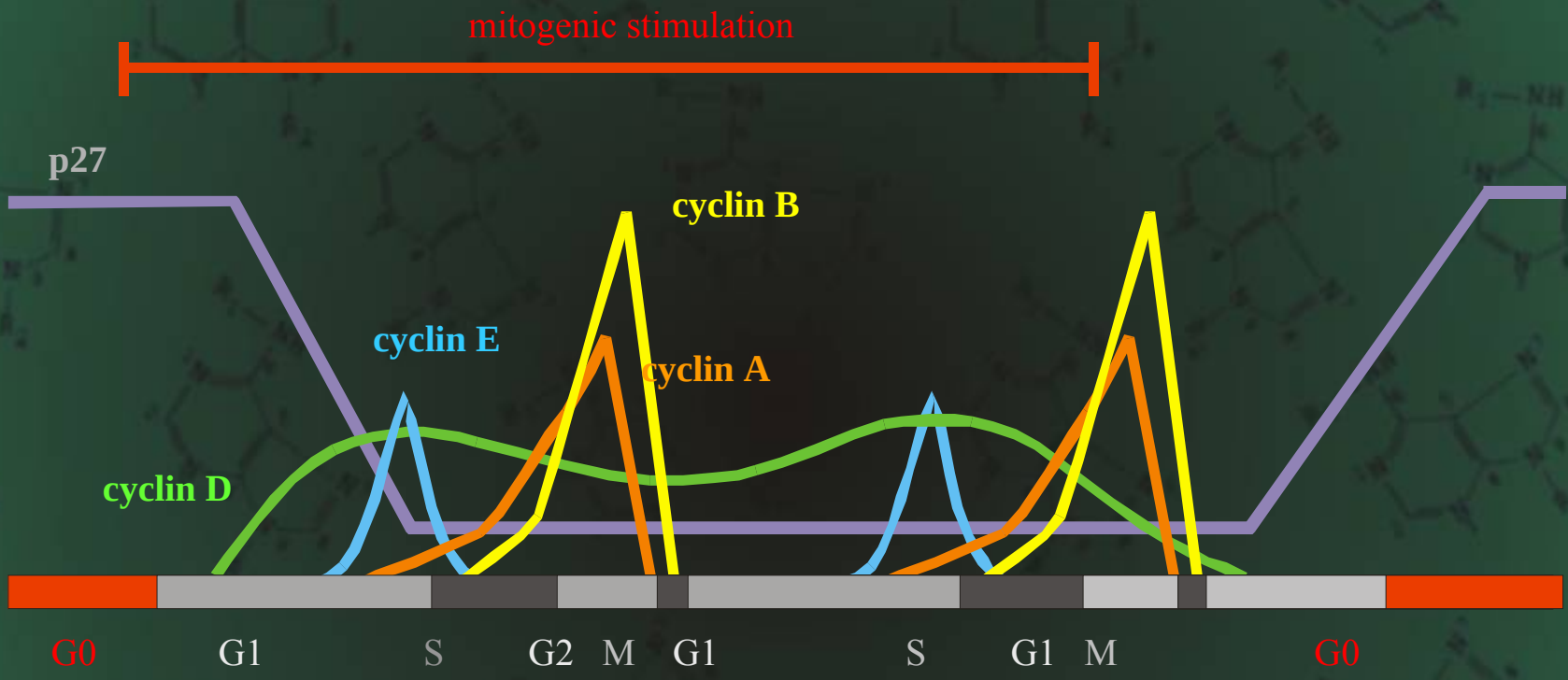

CDK inhibition

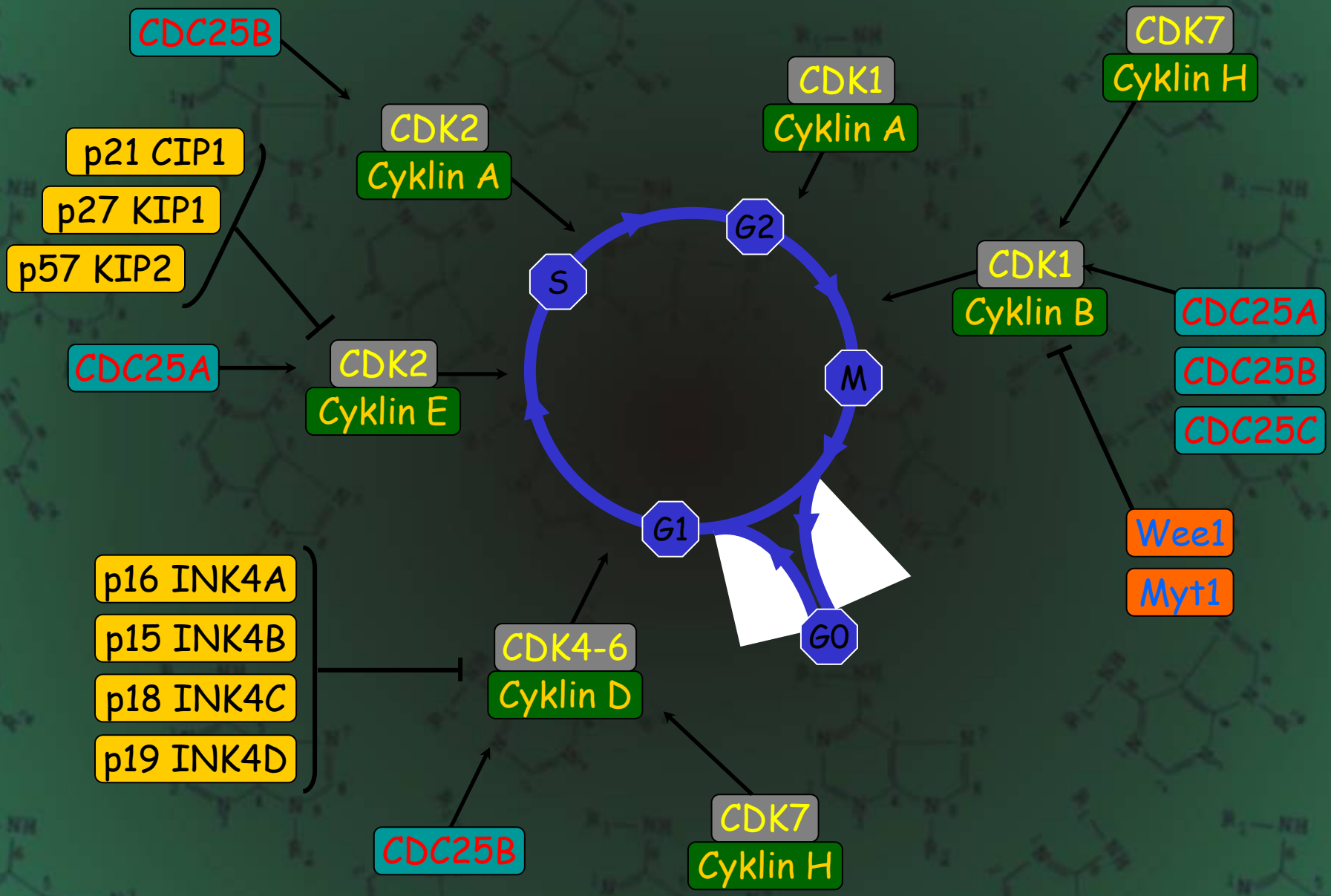

Cell cycle and cancer

c-myc, cyclin E, cyclin A, thymidin kinase, thymidylate synthase, DNA pol α, ...

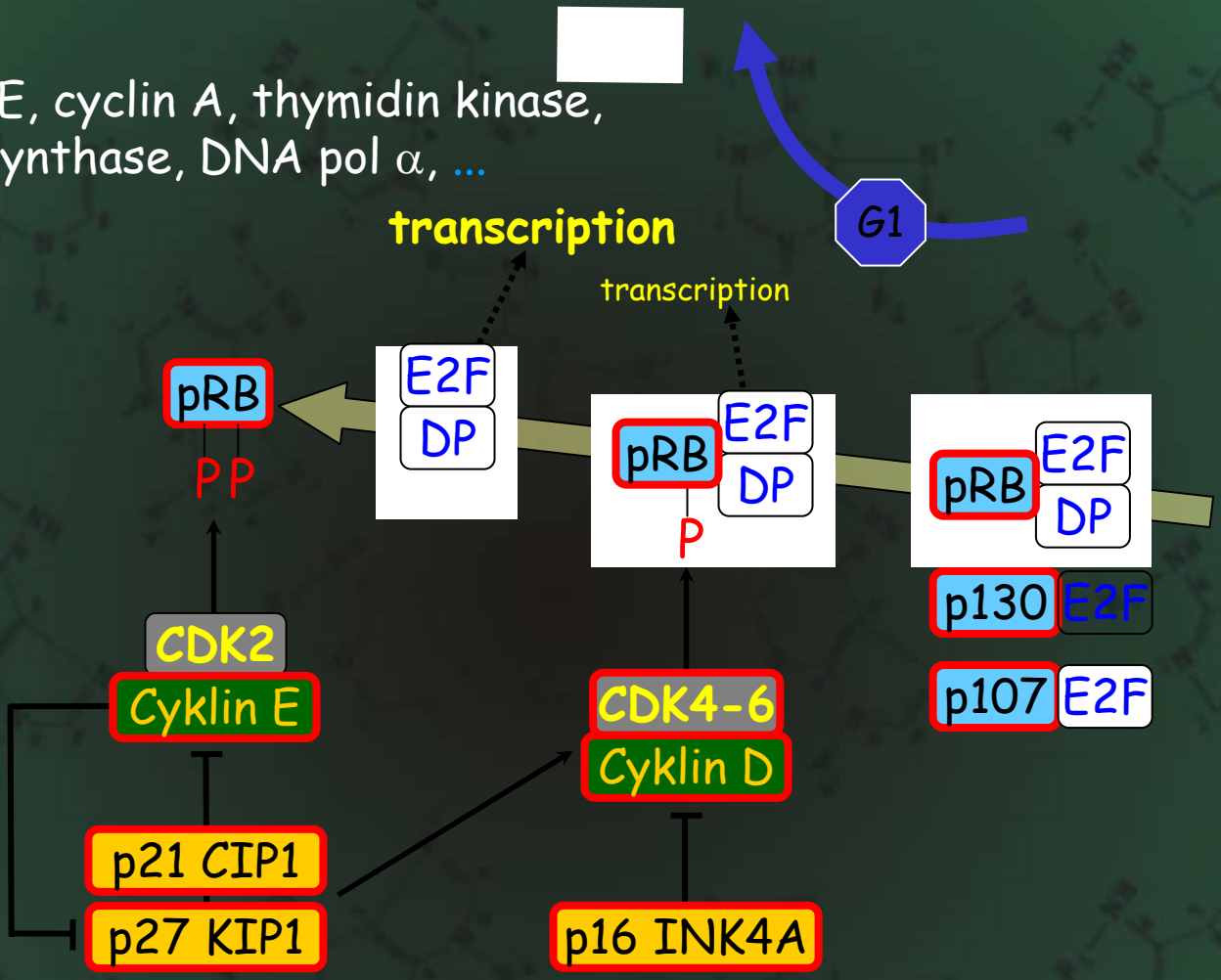

Stabilization of p53/induction of p21

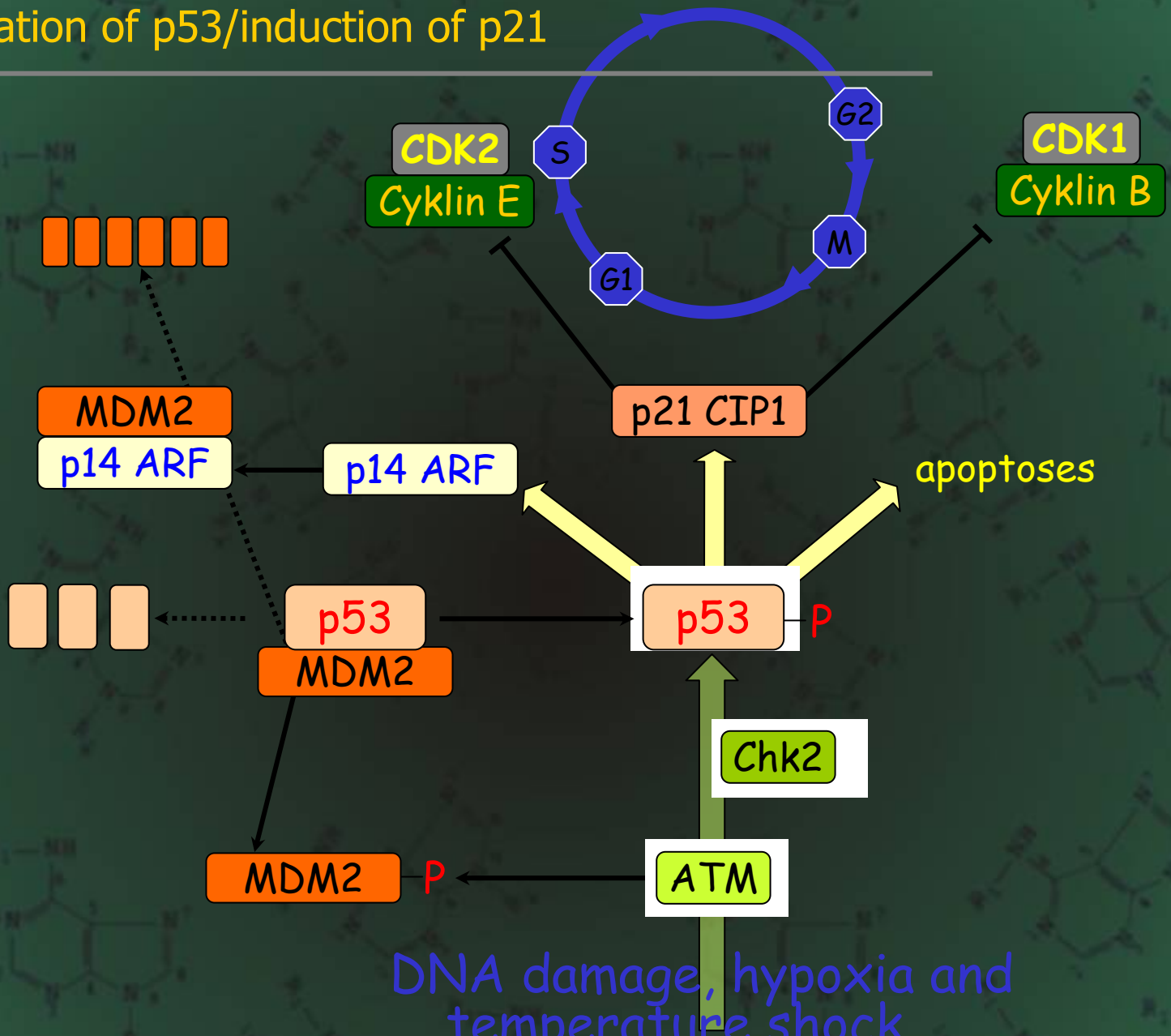

STRESS

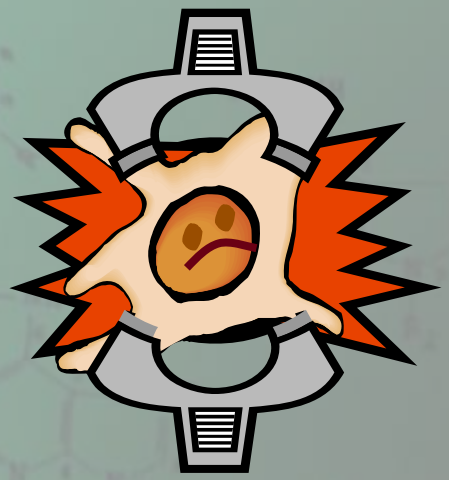

DNA damage
mitotic aparatus
oxidative stress
starvation, hypoxia

p53

Transcription factor

p53

Level

DNA binding ability

Interaction with transcrip. apparatus

Cell cycle block
Reparation of damage

p21 ,14-3-3σ
Gadd45, p53R2

Apoptosis

Bax, PUMA, NOXA
Fas, DR-5,
CD45, AIP1, PTEN
Scotin, PIG3

Acquired Mutation

Chemotherapy
Radiotherapy

Genetic instability
(BRCA mutation)

Embryonic Mutation

17p

LI-FRAUMENY
SYNDROM

Loss of 1. allele

Genetic instability
„Gain of function“
Dominant ngative effect

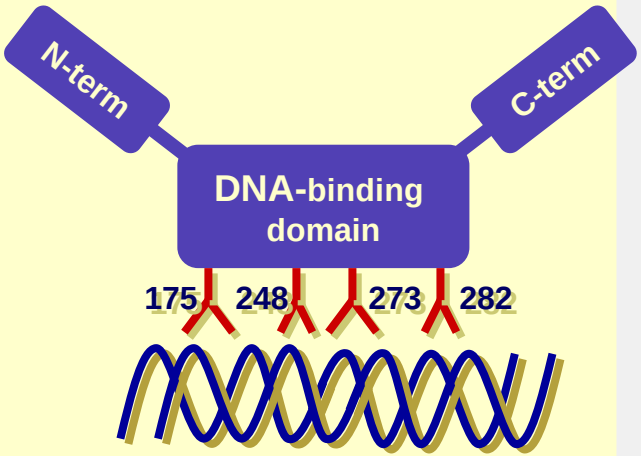

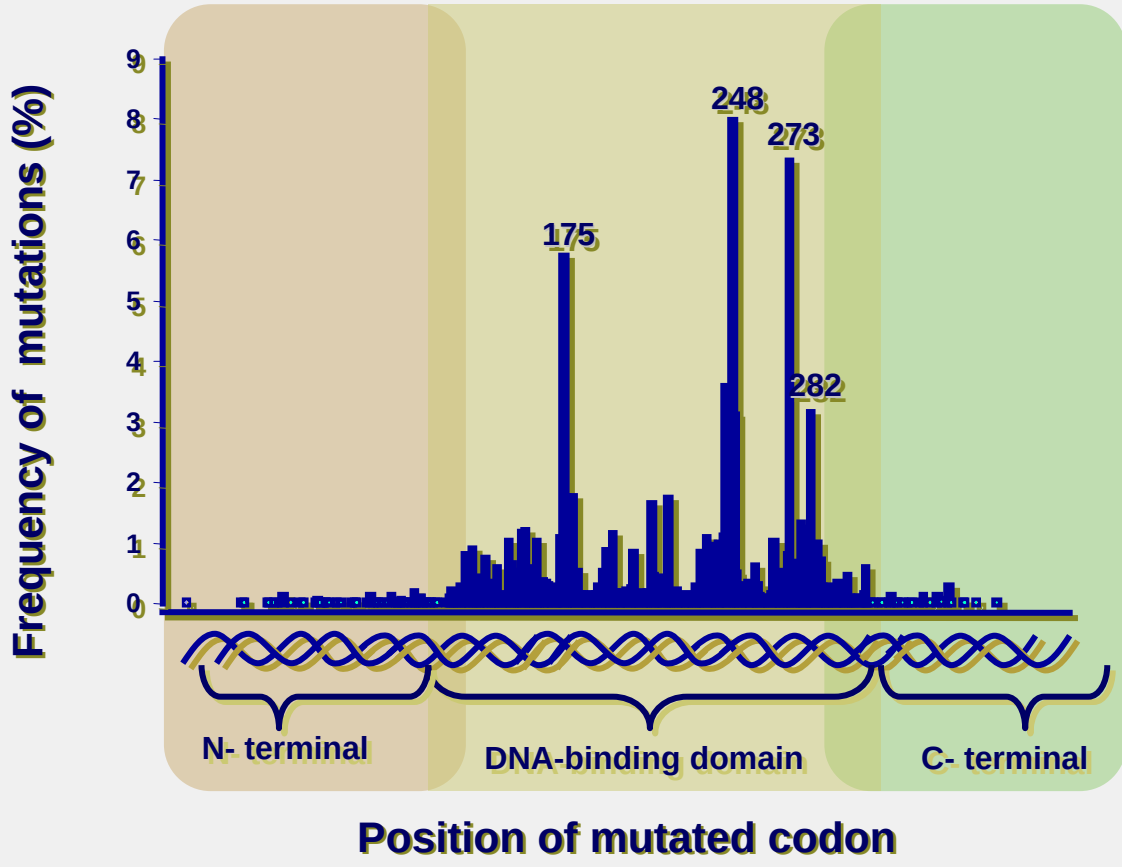

p53 signalling

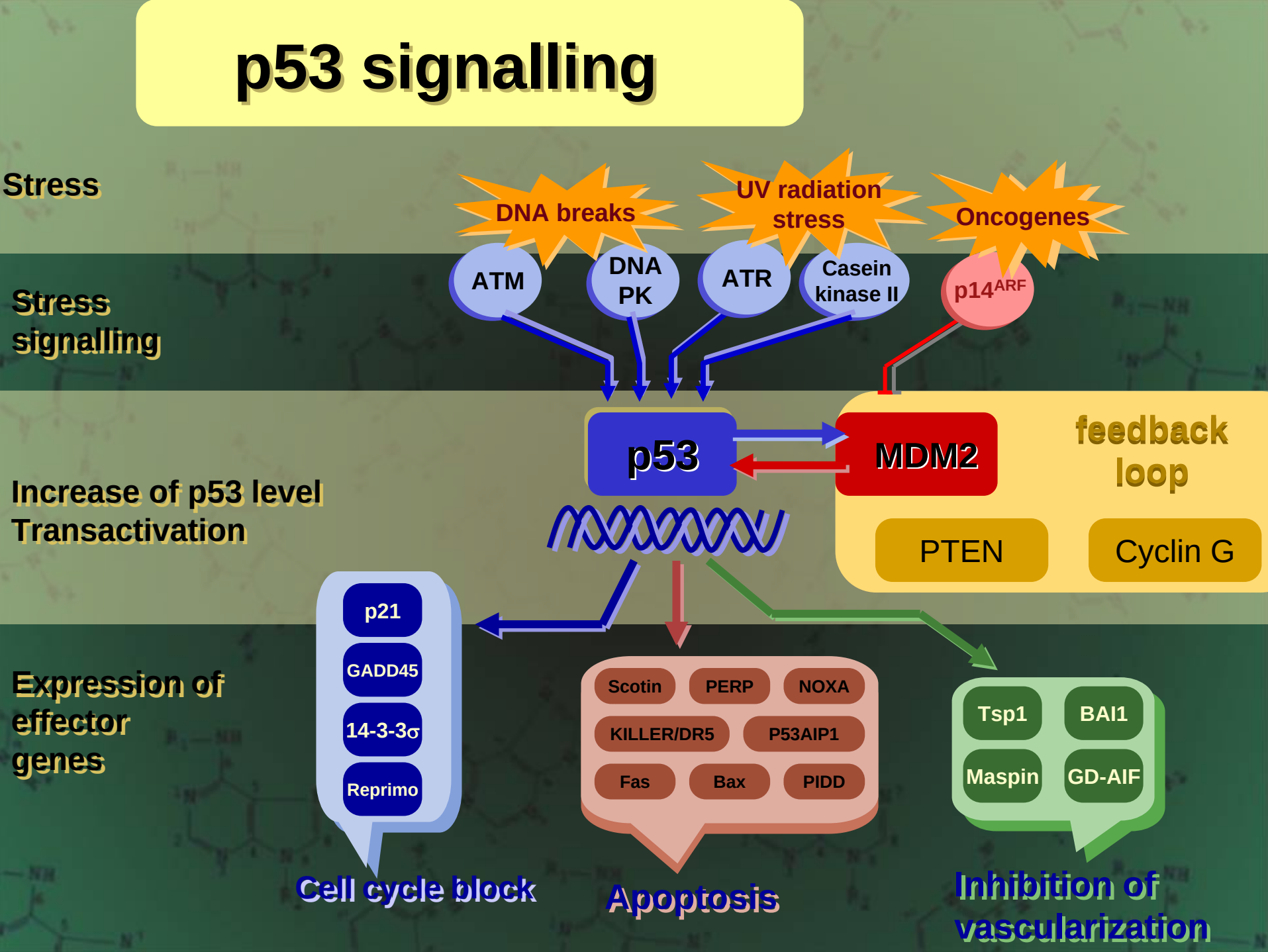

CDK's and cell division cycle

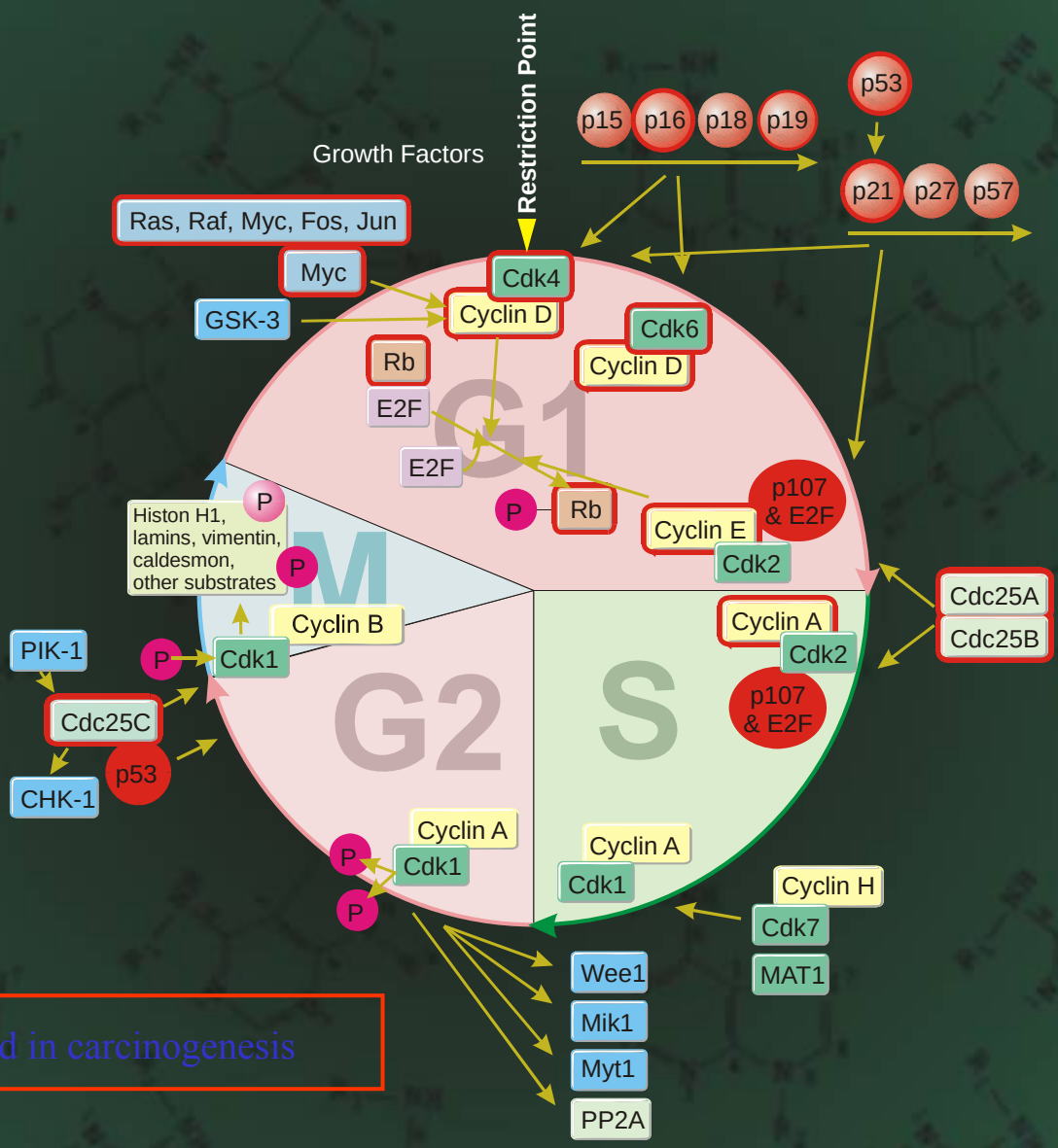

Proteins implicated in carcinogenesis

Microtubular arrays during cell cycle progression in plant cells

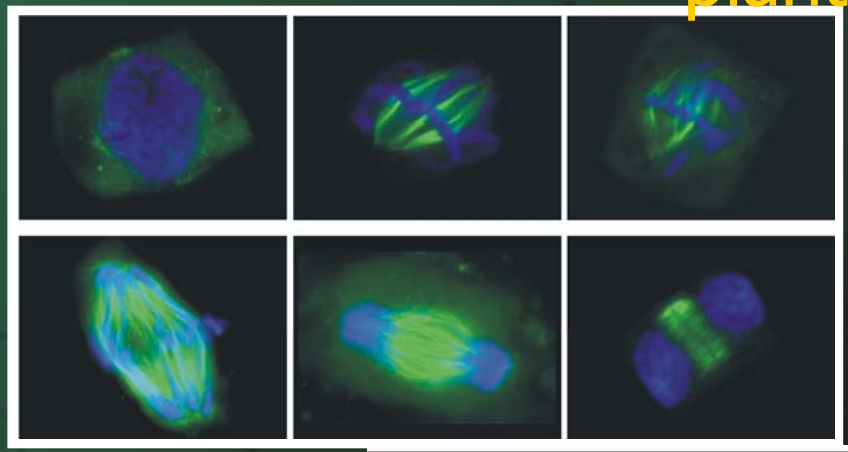

CDKB1/2
PPTALRE
PPTTLRE
motifs

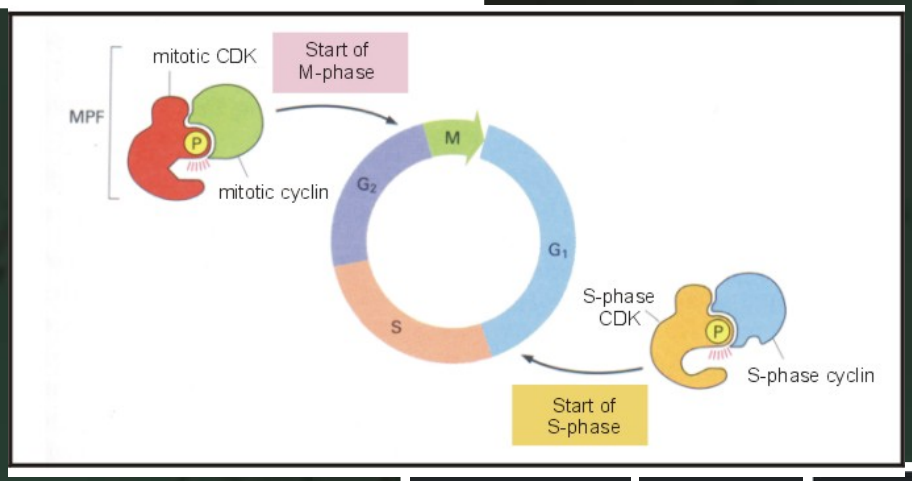

CDKA
PSTAIRE
motif

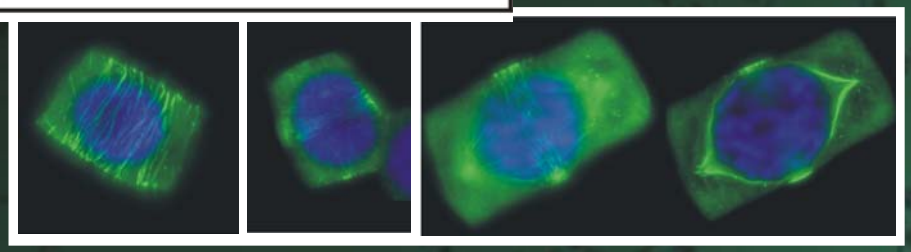

G1/S regulatory mechanisms in plant cells

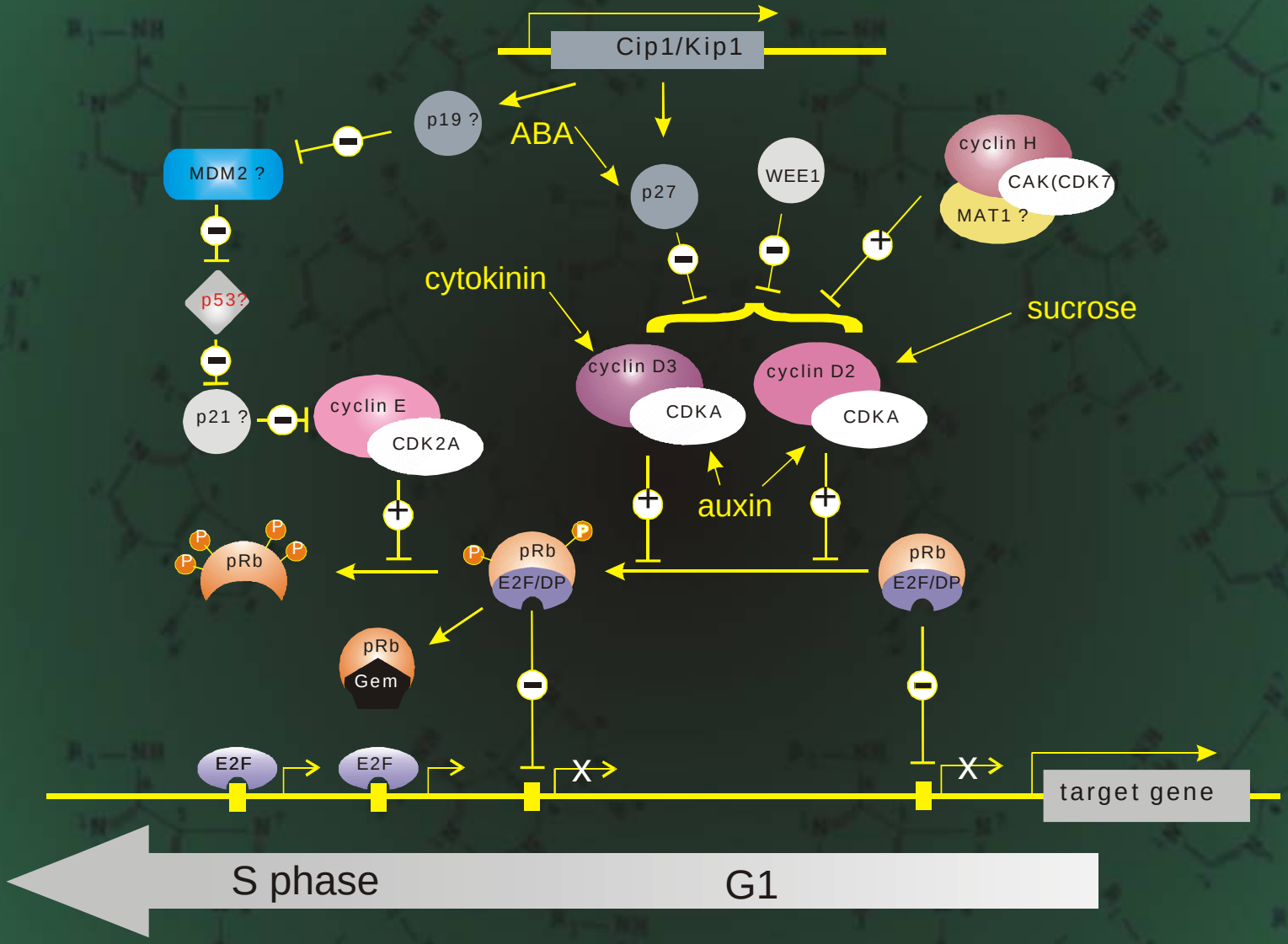

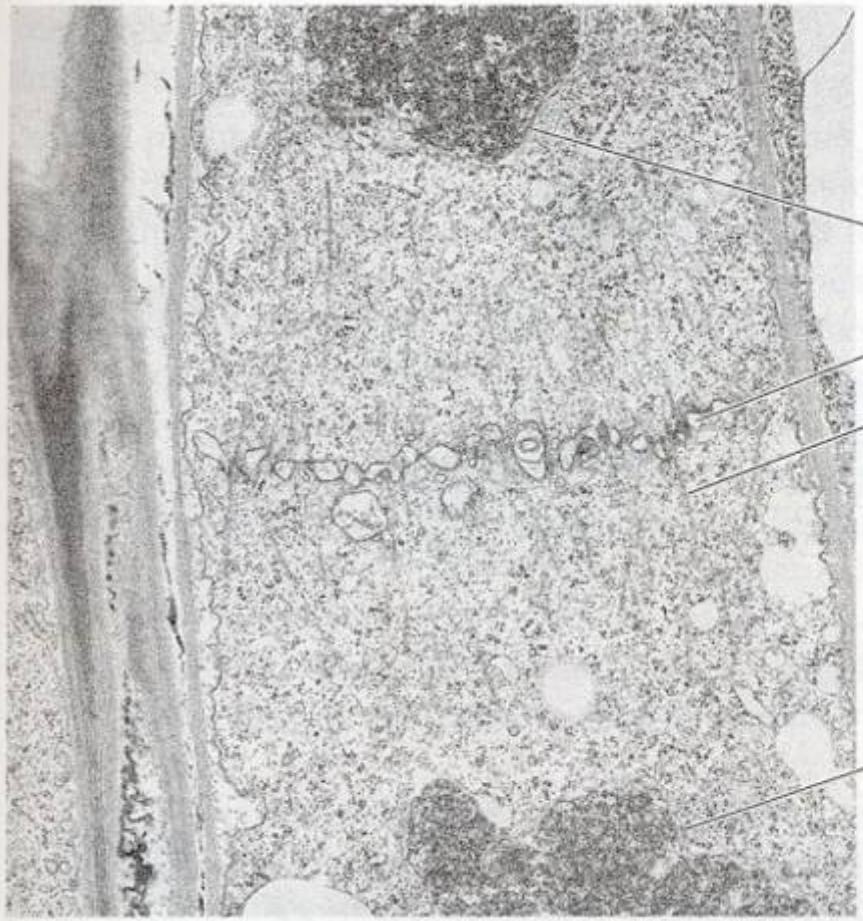

FIGURE 1.25 Electron micrograph of a cell plate forming in a maple seedling (10,000×). (© E. H. Newcomb and B. A. Palevitz/Biological Photo Service.)

the two chromatids of each replicated chromo
which were held together at their kinetochore
separated and the daughter chromosome
pulled to opposite poles by spindle fibers.

At a key regulatory point early in G_1 of th
cycle, the cell becomes committed to the init
of DNA synthesis. In yeasts, this point is
START. Once a cell has passed START, it is
versibly committed to initiating DNA synthes
completing the cell cycle through mitosis
cytokinesis. After the cell has completed mito
may initiate another complete cycle (G_1 th
mitosis), or it may leave the cell cycle and dif

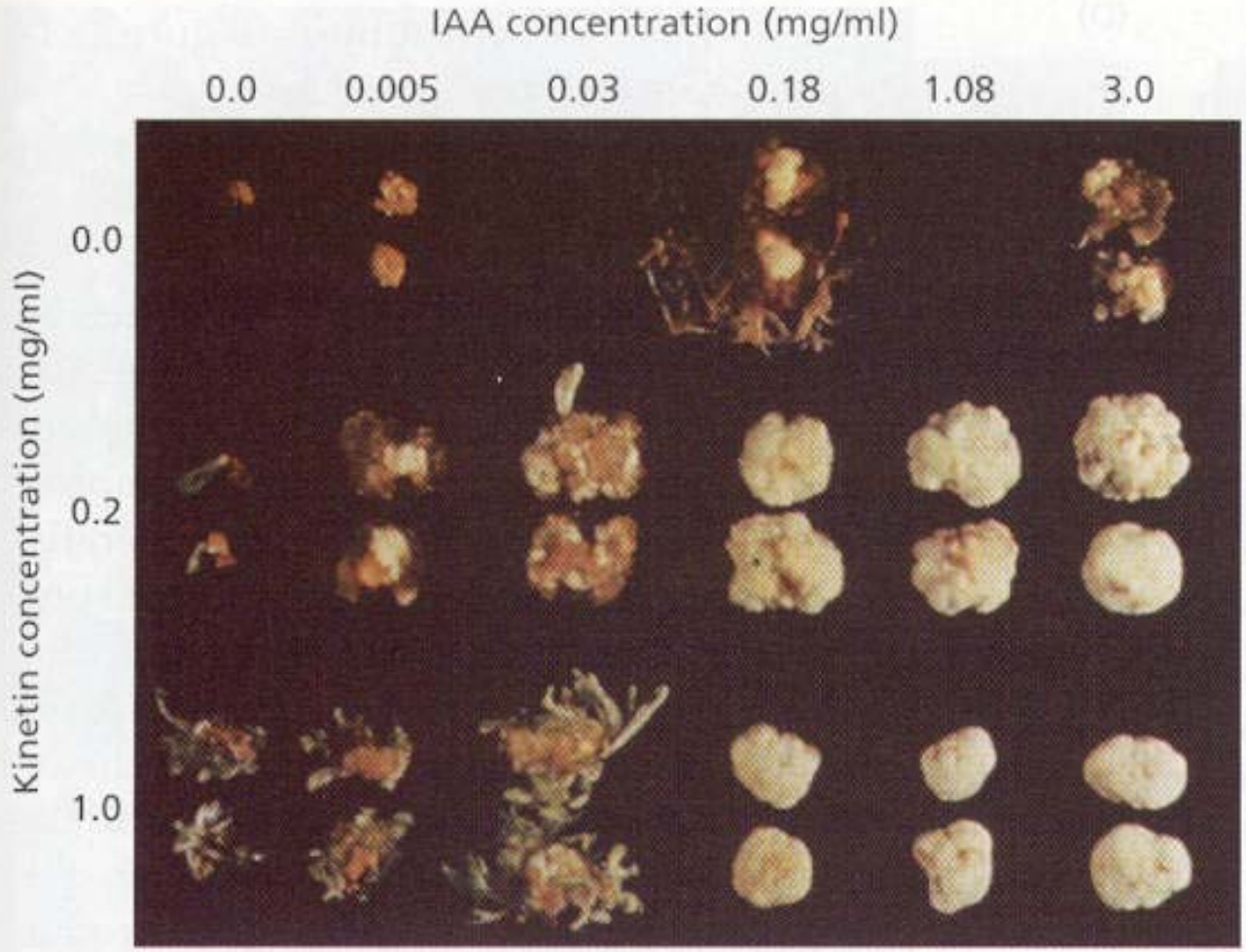

FIGURE 21.13 The regulation of growth and organ formation in cultured tobacco callus at different concentrations of auxin and kinetin. At low auxin and high kinetin concentrations (lower left) buds developed. At high auxin and low kinetin concentrations (upper right) roots developed. At intermediate or high concentrations of both hormones (middle and lower right) undifferentiated callus developed. (Courtesy of Donald Armstrong.)

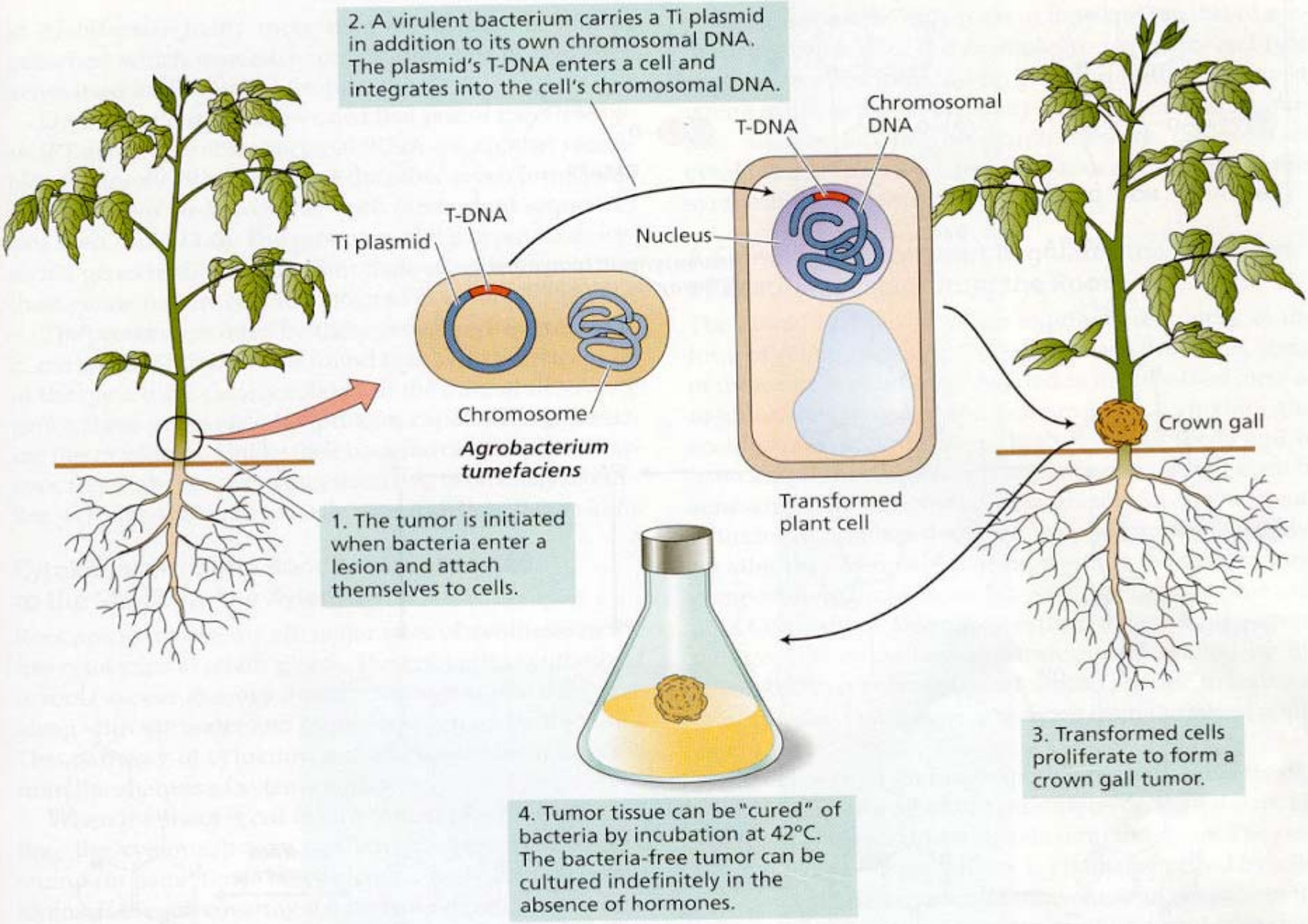

FIGURE 21.4 Tumor induction by *Agrobacterium tumefaciens*. (After Chilton 1983.)

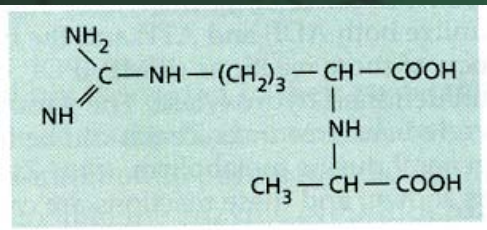

Octopine

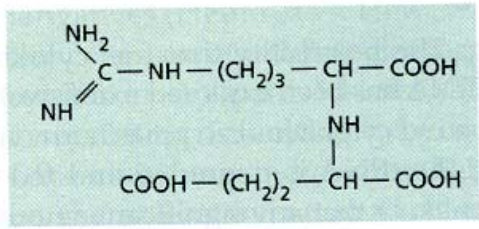

Nopaline

FIGURE 21.5 The two major opines, octopine and nopaline, are found only in crown gall tumors. The genes required for their synthesis are present in the T-DNA from *Agrobacterium tumefaciens*. The bacterium, but not the plant, can utilize the opines as a nitrogen source.

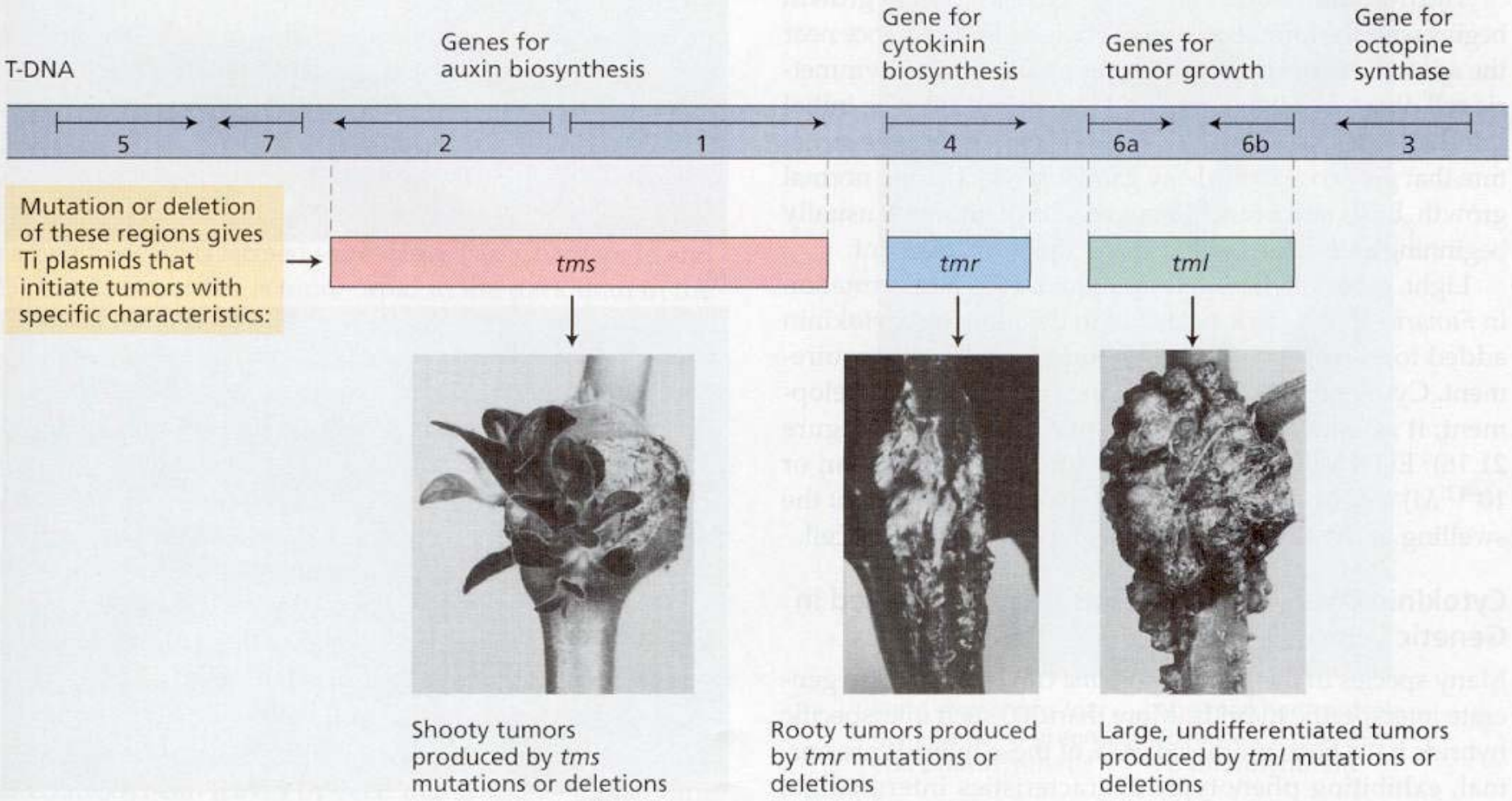

FIGURE 21.14 Map of the T-DNA from an *Agrobacterium* Ti plasmid, showing the effects of T-DNA mutations on crown gall tumor morphology. Genes 1 and 2 encode the two enzymes involved in auxin biosynthesis; gene 4 encodes a cytokinin biosynthesis enzyme. Mutations in these genes produce the phenotypes illustrated. (From Morris 1986, courtesy of R. Morris.)